QUANTITATIVE ANALYSIS OF DENDRITIC SPINE PLASTICITY USING IMAGE REGISTRATION IN TIME SERIES IMAGES

A thesis
submitted in partial fulfilment of the requirement for the Degree of
Master of Computer Science and Engineering
of
Jadavpur University
By

Ranit Dey
Registration No.: 140750 of 2017-2018
Examination Roll No.: M4CSE19019

Under the Guidance of
Prof. Subhadip Basu

Department of Computer Science and Engineering
Jadavpur University, Kolkata-700032
India
2019

FACULTY OF ENGINEERING AND TECHNOLOGY
JADAVPUR UNIVERSITY

Certificate of Recommendation

This is to certify that the dissertation entitled "Quantitative Analysis of Dendritic Spine Plasticity using Image Registration in Time Series Images" has been carried out by Ranit Dey (University Registration No.: 140750 of 2017-2018, Examination Roll No.: M4CSE19019) under my guidance and supervision and be accepted in partial fulfilment of the requirement for the Degree of Master of Computer Science and Engineering. The research results presented in the thesis have not been included in any other paper submitted for the award of any degree in any other University or Institute.

_____

Prof. Subhadip Basu (Thesis Supervisor)
Department of Computer Science and Engineering
Jadavpur University, Kolkata-32

Countersigned

_____

Prof. Mahantapas Kundu
Head, Department of Computer Science and Engineering,
Jadavpur University, Kolkata-32.

_____

Prof. Chiranjib Bhattacharjee
Dean, Faculty of Engineering and Technology.
Jadavpur University, Kolkata-32.

FACULTY OF ENGINEERING AND TECHNOLOGY
JADAVPUR UNIVERSITY

Certificate of Approval*

This is to certify that the thesis entitled "Quantitative Analysis of Dendritic Spine Plasticity using Image Registration in Time Series Images" is a bona-fide record of work carried out by Ranit Dey in partial fulfilment of the requirements for the award of the degree of Master of Computer Science and Engineering in the Department of Computer Science and Engineering, Jadavpur University during the period of September 2017 to June 2019. It is understood that by this approval the undersigned do not necessarily endorse or approve any statement made, opinion expressed or conclusion drawn therein but approve the thesis only for the purpose for which it has been submitted.

_____

Signature of Examiner 1
Date:

_____

Signature of Examiner 2
Date:

*Only in case the thesis is approved

FACULTY OF ENGINEERING AND TECHNOLOGY
JADAVPUR UNIVERSITY

Declaration of Originality and Compliance of Academic Ethics

I hereby declare that this thesis entitled "Quantitative Analysis of Dendritic Spine Plasticity using Image Registration in Time Series Images" contains literature survey and original research work by the undersigned candidate, as part of his Degree of Master of Computer Science & Engineering.

All information has been obtained and presented in accordance with academic rules and ethical conduct.

I also declare that, as required by these rules and conduct, I have fully cited and referenced all materials and results that are not original to this work.

Name: Ranit Dey

Registration No: 140750 OF 2017-18

Examination Roll No.: M4CSE19019

Thesis Title: Quantitative Analysis of Dendritic Spine Plasticity using Image Registration in Time Series Images

_____

.

Signature with Date

Acknowledgement

I would like to start by thanking the holy trinity for helping me deploy all the right resources and for shaping me into a better human being. I would like to express my deepest gratitude to my advisor, **Prof. Subhadip Basu**, Department of Computer Science and Engineering, Jadavpur University for his admirable guidance, care, patience and for providing me with an excellent atmosphere for doing research. Our numerous scientific discussions and his many constructive comments have greatly improved this work.

Words cannot express my indebtedness to **Prof. Mita Nasipuri**, Department of Computer Science and Engineering, Jadavpur University for her amazing guidance and supervision. I am deeply grateful to her for the long discussions that helped to enrich the technical content of this manuscript. I would like to thank **Prof. Ram Sarkar**, Department of Computer Science and Engineering, Jadavpur University, for helping me to deal with the problem related to image binarization.

I would like to thank **Dr. Jakub Wlodarczyk,** Department of Molecular and Cellular Neurobiology, Nencki Institute of Experimental Biology, Warsaw, Poland for providing the essential data for our research without which we can't test our method's efficiency.

Among the seniors I am deeply grateful to **Mr. Nirmal Das** for his guidance and supervision throughout the project work. Without his enthusiasm, encouragement, support and continuous optimism this thesis would hardly have been continued. I would like to thank **Mr. Anup Kumar Halder** educating me about Mendeley, which has proved to be an indispensable tool

to site research papers and providing the template for this thesis. I am highly grateful to **Mr. Azhar Uddin Molla** who taught me to about digital topology and skeletonization in image processing and shared his valuable technical knowledge.

I am also thankful to my friends **Mr. Sourav Dutta, Ms. Suchismita Ghosh, Mr. Aritra Nayak, Mr. Gaurab Ghosh, Mr. Swastik Biswas** and **Mr. Tapas Chakraborty** who were always present to motivate me.

Most importantly none of this would have been possible without the love and support of my family. I extend my thanks to my parents, especially to my mother whose forbearance and whole-hearted support helped this endeavor succeed.

This thesis would not have been completed without the inspiration and support of a number of wonderful individuals — my thanks and appreciation to all of them for being part of this journey and making this thesis possible.

Ranit Dey

Registration No: 140750 OF 2017-18
Exam Roll No.: M4CSE19019

Department of Computer Science & Engineering,
Jadavpur University

Contents

List of Figures

CHAPTER 1

INTRODUCTION

It is very much known to us that human beings are subject to various alterations both mentally and physically right from birth to adulthood. Plethora of perceptual, cognitive and motor functions mature over the course of 2 decades following birth. To have a good understanding of such developmental processes, merely studying behavioral changes is not enough; simultaneous investigation of the evolution of the brain is surely going to make way for a more comprehensive understanding. Here, it is of utmost significance to consider the development of the brain specifically from the perspectives of "structure" and "function" because both of them mature slowly. **Neuroimaging** or **brain imaging** is the usage involving various methodologies to model the structure, function or pharmacology of the nervous system.

A **dendritic spine** that protrudes from a neuron's **dendrite** is a small membranous protrusion that usually receives input from a single axon at the synapse. **Dendritic spines** act as the storage site for synaptic strength and helps in the transmission of electrical signals to the neuron's cell body. Dendritic spines are by nature "plastic", which means spines change significantly in shape, number and volume in very short time courses. Spines reveal remarkable morphological plasticity not only during the course of development but also in the adult brain. Theoretically speaking morphological plasticity of dendritic spines is extremely significant for learning and memory and spine morphological abnormalities relate to neurological disorders such as mental retardation and schizophrenia. The monitoring of dendritic spines morphological changes poses a major challenge in neuroscience studies. The variations of spine density and/or morphology are indicators of the cellular processes involved in neural plasticity underlying learning and memory and are symptomatic in neuropsychiatric disorders. Quantitative **spine plasticity** analysis can be done when images at different timestamps are available and it can help us to closely monitor the morphological plasticity of spines. Visualization and analysis of dendritic spines in time series images is the major focus of this report and state of the art technologies and algorithms have been used for the same.

1.1 HISTORY OF NEUROIMAGING

Neuroimaging or **brain imaging** involves incorporating different approaches to model the structure of the brain, its function and pharmacology of the nervous system. It is a brand new discipline within medicine, neuroscience and psychology [1] where extensive research is going on. **Neuroimaging** can be classified into two categories: (1) **Structural Imaging** dealing with structure of the nervous system and the diagnosis of gross (large scale) intracranial disease (such as a tumor) and injury. (2) **Functional Imaging** used for the diagnosis of metabolic diseases and injuries (or lesions) in a more sophisticated way (such as Alzheimer's disease) and also for neurological and cognitive psychology research and building brain-computer interfaces. Functional Imaging enables to visualize the information processing centers in the brain to be visualized directly which causes the area of the brain in concern to increase **metabolism** and "light up" during the scan. A major contentious application of neuroimaging has been researching "thought recognition" or mind-reading.

The first landmark in the history of neuroimaging finds its way back to the great neuroscientist Angelo Mosso who was the inventor of the 'human circulation balance', which was able to non-invasively measure the redistribution of blood during psychological and intellectual activity [2]. However, Mosso's experiments and the working details of this balance remained largely out of sight as stated by William Jones in 1980 until the recent discovery of the original instrument as well as Mosso's reports by Stefano Sandrone and colleagues. [3]

Walter Dandy an American neurosurgeon in the year 1918 introduced the technique of **ventriculography**. The acquisition of X-ray images involving the ventricular system inside the brain was done by injection of filtered air directly into one or both lateral ventricles of the brain. It was also observed by Dandy that air introduced into the subarachnoid space via lumbar spinal puncture could enter the cerebral ventricles and also demonstrate the cerebrospinal fluid compartments around the base of the brain and over its surface. The method was called **pneumoencephalography**. In the year 1927 Egas Moniz brought into use the concept of **cerebral angiography**, whereby blood vessels (normal and abnormal) in and around the brain could be visualized with utmost precision. In the early 1970s, computerized axial tomography (CAT or CT scanning) was introduced by Allan McLeod Cormack and Godfrey Newbold Hounsfield and greatly detailed anatomic images of the brain became available for diagnostic and research purposes. Cormack and

Hounsfield won the 1979 Nobel Prize for Physiology or Medicine for their work. After the inauguration of CAT in the early 1980s, the development of radioligands allowed single photon emission computed tomography (SPECT) and positron emission tomography (PET) of the brain. Very much at the same time, magnetic resonance imaging (MRI or MR scanning) was developed by researchers including Peter Mansfield and Paul Lauterbur, who were the Nobel Prize winners for Physiology or Medicine in 2003.

There are several brain imaging techniques few of which are discussed as follows:

- **Computed Axial Tomography** (CAT) scanning typically uses a series of x-rays of the head taken from many separate directions and is used for rapidly visualizing brain lesions. Finally an X-ray image is produced after processing of data using a form of tomography in which a computer controls the motion of the X-ray source and detectors.
- **Diffuse Optical Tomography** (DOT) is a medical imaging modality that incorporates the usage of infrared light to produce images of the body. The method measures the optical absorption of haemoglobin, and relies on the absorption spectrum of haemoglobin varying with its oxygenation status.
- **Magnetic Resonance Imaging** (MRI) being a medical imaging technique uses magnetic fields and radio waves and produces great quality 2D or 3D images of brain structures not using ionizing radiation (X-rays) or radioactive tracers.
- **Event-related Optical Signal** (EROS) making usage infrared light through optical fibers to measure changes in optical properties of active areas of the cerebral cortex. EROS being a brain-scanning technique takes advantage of the scattering properties of the neurons themselves and thus provides a much more direct measure of cellular activity.
- **Positron Emission Tomography** (PET) can measure emissions from radioactively labeled metabolically active chemicals that have been injected into the bloodstream. The emission data are computer-processed to produce 2D or 3D images of the distribution of the chemicals throughout the brain.
- **Confocal Laser Scanning Microscopy** (**CLSM**) is used for enhancing optical resolution and contrast of a micrograph by means of using a spatial pinhole to block out-of-focus light in image formation.[8] Capturing multiple two-dimensional images at different depths in a sample enables the reconstruction of three-dimensional structures (a process known as optical sectioning) within an object.

1.2 DENDRITIC SPINE "PLASTICITY" AND RELATION WITH NEURODEGENERATIVE DISEASES

Dendritic spines are actin rich small protrusions that emerge from the dendrites of neurons. Most excitatory synapses in the brain are found on spine heads. Typically, a spine consists of a bulbous head, volume 0.001–1 μm^3, at the end of a thin spine neck, diameter around 0.1 µm. A 100 µm length dendrite can contain several hundred spines. The human cerebral cortex is thought to contain in the order of 10^{14} spines! Dendritic spines serve as a storage site for synaptic strength and help transmit electrical signals to the neuron's cell body.

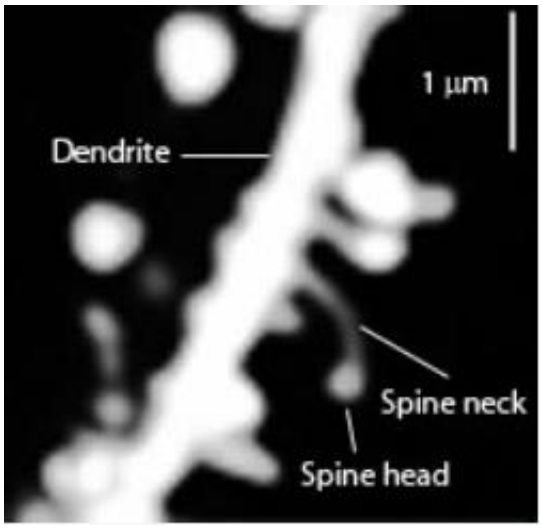

Figure 1.1 Spiny dendrite of a **striatal** medium spiny neuron.

All spines contain a postsynaptic density, an electron-dense thickening where the presynaptic axon contacts the spine. The postsynaptic density is made up of neurotransmitter receptors, ion channels, scaffolding proteins and signaling molecules. Polyribosomes are frequently present in the spines, and are hypothesized to be sites of local protein synthesis. An actin-based cytoskeleton provides the means for structural organization as spines mostly lack microtubules and intermediate filaments. If we probe deeper into the development of dendritic spines in neurons (spinogenesis) we'll see that initially a long thin thread like form called a **filopodium** which are thought to be spine precursors is built having long neck and no head. As time progresses Filopodia is replaced by **thin** spines which is characterized by long head and small neck, **stubby** spines with no neck or short neck and relatively mature **mushroom** shaped spines having long neck and large bulbous head. Synaptic activity very much influences spine morphology and

stabilization the most mature spines being the mushroom spines containing neurotransmitter receptors and a post synaptic density (PSD).

If we consider the mammalian brain co-ordination of neurons takes place via exchange of electro-chemical impulses which has many functions like cognitive perception, memory creation and retention. Spine morphology is considered to have a significant role in the cognitive process, such as learning through acquiring information and memory formation i.e. long term information retention. Dendritic spines are very "plastic" which means that there is alteration in shape, volume and number with time. Dendritic spines mainly have an actin skeleton, they are dynamic by nature and the majority of spines change their shape within seconds to minutes because of the dynamicity of actin remodeling. Motivation, learning and memory is implicated by **Spine plasticity**. The functional interaction between neuronal activity and different signaling pathways can produce new spines and affect spine maturation and stabilization/pruning, the processes which are essential for memory and learning. In general long-term memory is mediated in part by the growth of new dendritic spines (or the enlargement of pre-existing spines) to reinforce a particular neural pathway. Dendritic spines being plastic structures whose lifespan is influenced by input activity [4] spine dynamics may play a major role in the maintenance of memory over a lifetime. During high stress or pathological condition spine dynamics put forward some anomalies like increase or decrease in spine numbers, puerile structure of spine, mitigation of size, highly variable spine density and abnormal spine formation. While conducting research on neurological diseases and lesions further light is shed on the nature and importance of spine turnover. After the occurrence of a stroke, an increase in structural plasticity occurs near the trauma site and a considerable enhancement from control rates in spine turnover has been observed [5]. Major Cognitive disorders such autism, intellectual disability, and fragile X syndrome, may be a result from abnormalities in dendritic spines, especially the count of spines and their maturity. The ratio of matured to immature spines is important in their signaling, as immature spines have impaired synaptic signaling. Fragile X syndrome is characterized by an overabundance of immature spines that have multiple filopodia in cortical dendrites. Therefore, it is of utmost importance to have a deep understanding of the dynamics and morphology of dendritic spines which are hampered in several neurodegenerative diseases.

1.3 IMAGING MODALITIES

There has been immense advancement in biomedical imaging technologies. This has allowed visualization of multi-dimensional and multi-parameter data which has made a revolutionary impact on biomedical researchers and diagnostic radiology. **Medical Imaging** is in essence the method and process of forming visual representations of the interior of a body for clinical analysis and medical intervention, as well as the function of some organs or tissues. Medical imaging attempts to disclose internal structures hidden by the skin and bones, as well as for the diagnosis and treatment of diseases. Highly improved detectors, instrumentation and computing methods have transformed the various medical imaging modalities to be able to create an information warehouse for greater understanding of physiological processes and clinical management of critical diseases. Medical Imaging as a discipline in its widest sense is a part of biological imaging and incorporates radiology which uses the imaging technologies of X-ray radiography, computed technology (CT), Magnetic Resonance Imaging (MRI) and Positron Emission Tomography (PET). The data for our proposed method has been collected using confocal microscope so we'll focus on different microscopic imaging tools. Data acquired with various microscopic techniques provide a variable magnification and depth of field which established a comprehensive understanding of different biological function and pathological condition at cellular level. Microscopic imaging modalities includes fluorescence microscopy, confocal microscopy, multiphoton microscopy, atomic force microscopy and electron microscopy.

Confocal microscopy, most frequently **confocal laser scanning microscopy** (**CLSM**) or **laser confocal scanning microscopy**(**LCSM**), is an optical imaging technique for increasing optical resolution and contrast of a micrograph by means of using a spatial pinhole to block out-of-focus light in image formation. This technique is used appreciably in the scientific and industrial communities and the crucial typical applications are in life sciences, semiconductor inspection and materials science. In confocal microscopy, optical or fluorescent properties of a specimen is measured by blocking all out of focus light using a small pinhole i.e. only considering the light which is reflected from object in the focal plane i.e. a slim optical section of 3D plane. A confocal laser scanning microscopy (CLSM) incorporate a laser to scan over an object one pixel and one slice. CLSM is widely used in numerous science disciplines from cell biology to genetics and developmental biology. [9] It is also used in Quantum optics nano-crystal imaging and spectroscopy. CSLM can be useful to digitalize a comprehensive 3D image volume. Confocal microscopy can obtain high resolution slice by slice of ex-vivo or in-vivo cell. Confocal microscopy is used to investigate

structural and morphological properties of cells and differentiate between normal and odd cells for diagnosis. **Two-Photon Microscopy** is a slight alteration of confocal microscopy that greatly enhances imaging in thick living tissue, such as brain slices or in-vivo brains. In two-photon microscopy procedure a fluorophore can be excited by effectively absorbing two photons simultaneously and when this happens each contributes half the needed excitation energy to interact with the fluorophore. The main advantage of this method is that the near-simultaneous arrival of two photons is an extremely rare event, so fluorescence excitation is restricted to a narrow plane of focus within the specimen. This provides clearer images than traditional confocal microscopy, even in cases where relatively few fluorophores are present, because photons are only emitted from the excited fluorophores located at the focal plane.

Major advancements in fluorescence microscopy has been a major step towards the enhanced study of living cells. It can be used to have a proper understanding of cell structure and function. Multiphoton method has been developed following the tradition fluorescence microscopy, where fluorophores such as fluorescent proteins are exited using two or more photons. Multiphoton microscopy (MPM) is regarded as the method of choice for imaging of living, intact biological tissues on length scales from the molecular level through the whole organism. Additionally, multiphoton microscopy is uniquely suited to perform experimental measurements with minimal invasion over long periods of time, thereby providing exquisite detail of inherently dynamic biological processes having time scales from microseconds to days or weeks. As a result, vast quantities of data are becoming available to further enhance our understanding of complex biological interactions. Compared to similar optical imaging techniques, MPM holds inherent advantages for imaging living tissues by improving depth penetration and reducing photo damage. This is a direct result of employing near infrared (NIR) femtosecond lasers to generate observable nonlinear signals in the visible range. **Stimulated Emission Depletion** (**STED**) **microscopy** is one of the techniques that make up super-resolution microscopy. It creates super-resolution images by the selective deactivation of fluorophores, minimizing the area of illumination at the focal point and enhancing the achievable resolution of given system [6]. Electron microscopy allows to reconstruct the structure of biological objects in their native states in 3D with resolution of ~5nm.[7]

1.4 QUANTITATIVE ANALYSIS OF DENDRITIC SPINES AND ITS SIGNIFICANCE

Quantitative analysis of changes in dendritic spine morphology has become an interesting issue in contemporary neuroscience. Many physiological and pathological phenomena rely on brain plasticity, including learning and memory, epileptogenesis, drug addiction and post injury recovery. The quantitative analysis of spine morphology is therefore the essential problem. The morphology of spines is known to reflect their structure and function. Therefore, the morphology of spines is of relevance to many researchers who study the plasticity processes. In this work we have focused to quantitatively analyze morphological changes in individual spines in **time series** 2D images before and after chemically induced long-term potentiation. 3D microscopy helps us to acquire images and then processing the image is commonly used to study different biological objects at a different scale such as cells, neuron and tissue. Let's focus on what information gives us. It is very much possible to reconstruct a focused 2D image which can adequately represent all the information present in the 3D stack. To generate a 2D image from 3D stack a projection in the z direction is our principal need because it is possible to quantify the information retained which turns out to be maximum. Above 80 percent of the biologist community use MIP, to reduce a 3D stack into a single 2D image. MIP retrieves the level of maximum intensity along the z axis for each x, y position. The image of 3D stack is called the index map while the image made of intensity values corresponding to that index map is called the projection. MIP is widely adopted as it is the simplest method of z-projection, parameter free, fast and straightforward to use as it is implemented in NIH Fiji/ImageJ7 and in many other programs. Our dataset is generated by imaging different neuron from rat dissociated hippocampal cultures using a confocal light microscope, before and after chemically induced long-term potentiation (cLTP). Images have been captured for multiple time instants to identify the structural and morphological changes in the chemical solution over time. There are certain features in these time series 2D MIP images of dendritic spines analyzing which can help us to understand the spine morphology during neurodegenerative diseases like Alzheimer, Schizophrenia and Fragile X-syndrome (FXS) better. Different experiment shows during highly stress or pathological condition spine dynamics unveil some anomalies like loss or decrease in spine numbers, immature structure of spine, reduction of size, highly variable spine density, ectopic spine formation, sometimes highly increased spine number. Therefore, quantitative analysis of features like number of spines, total dendrite length, spine density, individual spine length, head width, neck length, etc. can help us to closely

monitor the morphological changes in dendritic spines during highly stress or pathological conditions. As these features vary a lot within a short span of time spine morphology and distribution is a critically important factor that still needs to be worked on properly as numerous neurological disorders such as mental retardation and schizophrenia are associated with spine morphological abnormalities. Therefore, the visualization and analysis of dendritic spines over time is critically important tool for researches on synaptic plasticity.

1.5 SIGNIFICANCE OF TIME SERIES IMAGES

The collection of images of a particular object that are acquired over a period of time is called **time series** images. Such a kind of procedure allows medical researchers the ability to monitor several different situations which may arise during a patient's life. For our work we have images of different neuron at different time instants from rat dissociated hippocampal cultures using a confocal light microscope, before and after chemically induced long-term potentiation (cLTP). Therefore, in these **time series** images it is our objective to track the morphological changes occurring in the dendritic spines over a period of time. This observable morphological changes in the spines is called **spine plasticity** which involves changes in shape and density of dendritic spines. Neuronal activity is responsible for the modification of spine morphology and how these modifications affect synaptic transmission and plasticity are intriguing issues. Indeed, the induction of long-term potentiation (LTP) or depression (LTD) is associated with the enlargement or shrinkage of the spine, respectively. This structural plasticity is mainly controlled by actin filaments, the principal cytoskeletal component of the spine. The figure 1.2 shows images of dendritic spines on 3 different timestamps T0, T1 and T2.

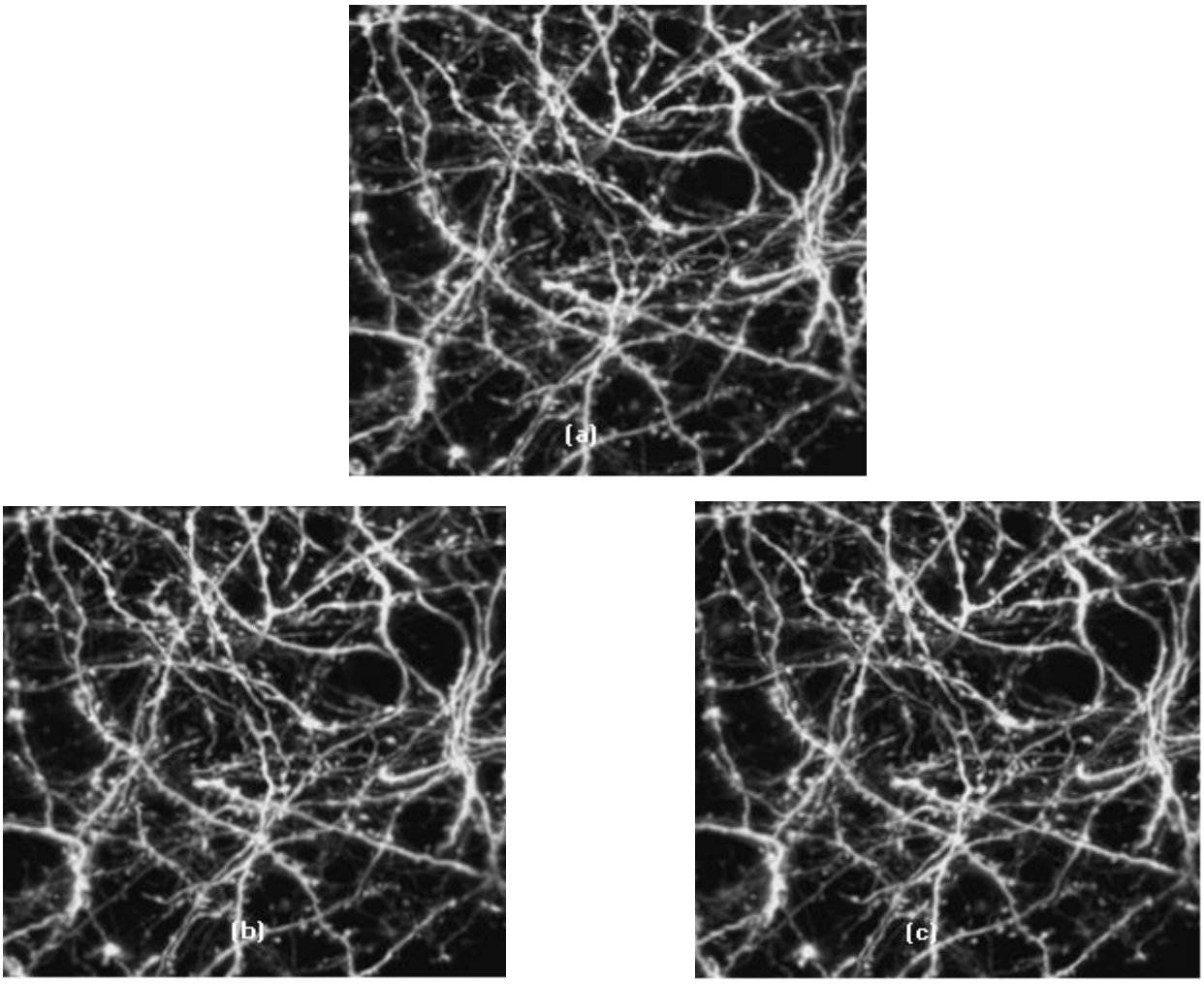

Fig 1.2 2D MIP images of dendritic spines at different time instants (a) MIP of cell at T0 (b) MIP of cell at T1 (c) MIP of cell at T2

1.6 SIGNIFICANCE OF IMAGE REGISTRATION

Image Registration is a defined as a process that overlays two or more images from various imaging equipment or sensors taken at different times and angles, or from the same scene to geometrically align the images for analysis. In medical imaging, registration enables to combine data from multiple modalities such as CT, MR, SPECT, or PET to obtain complete information about the patient. It can help to monitor tumor growth, to facilitate treatment verification, to improve interventions, or to compare patient's data to anatomical atlases. There are many registration methods and to be able to decide which method is the most appropriate for a given task and a dataset it is important to take into account issues

inherent to medical imaging, related to data types, to an acquisition process as well as to required accuracy and sensitivity to errors. In our approach Rigid Body Registration using Mutual Information has been done because it can spatially align time series images of different time instants. The main motive of our work is to track spine behavior in time series images which would be impossible if the spatial location of the spines is not properly aligned which is what we see in case of the data that we have before applying our image registration algorithm. Image registration helps in rectifying this misalignment.

1.7 MOTIVATION

Although much research work has been done so far in the field of dendritic spine analysis in case of 2D Maximum Intensity Projection (MIP) images but still there is a scope of improvement in Image Binarization, Skeletonization, Plasticity Analysis, etc. But almost no major work has been done in tracking spine behavior in 2D MIP images of dendritic spines at different time instants. The analysis of spine "plasticity" in 2D MIP images of different time stamps is of prime significance since spine dynamics during highly stress or pathological condition spine show some anomalies like loss or decrease in spine numbers, immature structure of spine, reduction of size, highly variable spine density, ectopic spine formation, and sometimes highly increased spine number. Spine plasticity is important for memory and learning. In the 2D MIP images taken at different timestamps there is little bit of misalignment which can be due to two or more images being clicked from various imaging equipment or sensors taken at different times and angles. *Image Registration* helps in rectifying this misalignment. After rectifying this alignment the segmentation procedure of dendrites and spines becomes possible in 2D MIP images of different time stamps. Therefore, quantitative features can be extracted like *spine area*, *spine length*, etc. which are utilized in plasticity analysis.

1.8 SCOPE OF THE WORK

The major focus of this thesis report is to provide fast two-dimensional (2D) analysis of dendritic spine plasticity in images of different time stamps using confocal light microscopy and two-photon microscopy images of dendritic spines of rat dissociated hippocampal cultures. Three-dimensional (3D) microscopy is used for image acquisition since a 3D stack contains all pieces of information needed to reconstruct a focused 2D image. Maximum Intensity Projection (MIP) used to create a 2D image from a 3D stack is often preferred as it retrieves the level of maximum intensity along the z axis for each x, y position. During image processing MIP of the confocal z-stack is used to convert the 3D stack image into a

2D image. *Gaussian de-noising* is performed on 2D MIP image for quality enhancement. *Image Registration* helps rectifying the misalignment between two images which might be due to the image acquisition scheme. Then segmentation of dendrite and spines has been done and spine features are calculated which are relevant to plasticity analysis.

1.9 ORGANIZATION OF THESIS

In *Chapter 1,* we discussed the basic introduction of dendritic spines and its importance in our memory generation and different pathological conditions. We have also discussed about dendritic spine plasticity and its relevance during neurodegenerative diseases. Some of the imaging modalities have also been discussed. A brief introduction to time varying (time series) images has also been provided and also the role of Image Registration has been explained.

In *Chapter 2,* a brief survey of different work that has been done so far to analyze the dendritic spines shape and nature has been presented and from this how we get our motivation of work.

In *Chapter 3,* a survey of different Image Registration techniques and explanation as to how they are classified has been provided. Then 2 algorithms have been proposed one being Skeletonization and the other one explains the Image Registration general procedure in detail. After that the our principle objective which was to rectify the misalignment in the images has been achieved through 2 state of the art algorithms which are Skeleton Based Registration and Pixel Based Registration respectively. The general idea behind these algorithms has been explained in detail and their performance has also been evaluated.

In *Chapter 4,* the various methodologies that have been adopted are explained. Firstly, the preprocessing method has been discussed. The Image Registration technique and how it helps to align the images has been explained along with the results obtained. The Dendrite and Spine Segmentation along with the pseudo code of the algorithm and results have been provided. Lastly how the features of individual spines like Spine Area, Spine Length, etc. are calculated have been elucidated.

In *Chapter 5*, basic explanation of the process of developing the GUI for Plasticity Analysis of Dendritic Spines using basic QT GUI module. The steps to use the GUI are also included here in this chapter.

In *Chapter 6,* an overall discussion of the work related to its advantage, shortcomings, future scopes are also discussed and concluded.

CHAPTER 2

LITERATURE SURVEY

This particular survey is mainly focused on experimental work that has done the analysis of the morphological consequences of hippocampal dendritic spines**.**

In the year 1973 it a discovery was made that brief tetanic stimulation produced a long lasting form of synaptic plasticity, long-term potentiation (LTP) that can last for hours or days in the mammalian hippocampus [9]. Since then, many researches have been done on LTP as a cellular model for information storage in the brain.

Hosokawa et al., [10] made a statistical analysis of changes in the length of individual spines using the confocal microscopy in conjunction with micro-drop application of Dil. They used confocal microscopy of hippocampal slices in which individual CA1 pyramidal cells were stained by a specially developed "DiI-microdrop technique." Synaptic potentiation was induced by "chemical LTP," produced by the application of a super fusion solution containing elevated Ca2+, reduced Mg2+, and tetraethyl ammonium. Using this experimental approach, the authors observed that a subpopulation of (small) spines extended, and they further reported that there was an increased range of angular displacement of spines in the potentiated tissue. All other parameters showed no significant changes. In particular, the appearance of completely new spines was a rare (and statistically insignificant) event.

Michele Papa *et al.,* [11] monitored development alternation in the dendritic spine in primary culture of hippocampal neurons using Confocal Laser Scanning Microscopy (CLSM). They observed the morphological changes of neurons over 4 weeks and increase in spine density about 170% from 1 to 3 weeks of the culture and decrease in spine density and the number of cell due to aging. Their studies lead to better understanding of the morphological changes in neuron.

In 1996 a study by Michele Papa *et al.,* [12] shows that the dendritic spine is a dynamic structure, highly responsive to the changes in the ambient condition. Their studies monitored the effect of dendritic spine in regulation of rise of postsynaptic Ca2+. The shorter spines have more impact on dendritic Ca2+.

J. Radley *et al.,* [13] examined the effect of repeated restraint stress on dendritic spine number in medial prefrontal cortex (PFC). They found that after exposure to repeated restraint stress a significant reduction in apical dendritic spine density of the medial PFC. This effect

was most pronounced at distances of 200lm from somata and on large diameter dendrites. From their experiment they suggested the effect of repeated restraint stress in medial PFC is highly selective.

In 2007 G. Kim *et al.,* [14] proposed that a fixation with the lower percentage of Paraformaldehyde (PFA) results in superior diffusion of lipophilic dye Dil along the neuronal membranes with adequate preservation of structural integrity. With this method a high quality of confocal images achieved which allowed distinctive synaptic morphology that are implemented in the process of structural synaptic plasticity. This method seems to be more suitable for structural analysis of spines rather than detailed measurement of dendritic branches.

A. Alvarez *et al.,* [15] reviews some of the spine detection and reconstruction methods and conclude that dendritic spines undergo changes in shape and size and their turnover rates decline with age.

U. Valentin Nägerl *et al.*, [16] proposed a technique that substantially improves the qualification of morphological parameters which play a critical role for the function and plasticity of synaptic connections.

Jan Tønnesen [17] used time lapse super-resolution STED imaging in combination with 2 photon glutamate uncaging, electrophysiology and simulations and FRAP measurements to investigate the dynamic link between nanoscale anatomy and compartmentalization in live spines of CA1 neurons in mouse brain slices. The STED images reveal structural details and a diversity of spine shapes and sizes.

An automated serial transmission microscopy process has been proposed by Yuriy Mishchenk *et al.,* [18] to densely reconstruct ssTEM four volumes of neuropils from the middle of the stratum radiatum in Rat hippocampus using automated registration and segmentation algorithm. Their results provide a guidance for reconstructing circuits with lower resolution methods but there is some uncertainty about the generalization beyond s. radiatum of the hippocampal area of CA1.

Won Chan Oh *et al.,* [19] proposed that low frequency glutamatergic activity at individual dendritic spines leads to spine shrinkage on CA1 neurons in the hippocampus. Their experiment shows that large spines have higher group I mGluR activity than small pieces.

In 2014 Rafael Yuste [20] viewed the dendritic spine behavior from the perspective of the circuit function and shows how spine would endow these circuits to function as neural networks.

Roberto Araya [21] use two photon calcium imaging of neocortical pyramidal neurons of mouse to analyze the correlation between the morphologies of spine activated under minimal synaptic simulation and excitatory postsynaptic potential they generate. They show that spike-timing simulation can induce synaptic potential and selectively shorten the length of the spine neck.

W. Christopher Risher *et al.,* [22] build a software named RECONSTRUCT that successfully conveyed the maturational shift in spine types during development in the mouse primary visual cortex. They use Golgi-cox staining protocol and acquired the image and import the z-stack into an image analysis program. There method confirmed both an increase in protrusion density with developmental age and changes in spine shape. There algorithm takes into account the length and width measurements of the analyzed spines. The major drawback of their method is the time required to stain and image the Golgi-stained slides. They have to manually sort the z-stack images to find dendritic segment for analysis. Another significant drawback of this software is the differences in spine classification from user to user as it is not user independent.

2016 Basu *et al.,* [23] proposed a semi-automated method named 2D-Span for quantitative analysis of spine morphological changes with reduced manual intervention. This tool is useful in a variety of applications involving large-scale annotation of dendritic spines for quick and accurate assessment of spine plastic changes. They used confocal light microscopic image of dendritic spines from disassociated hippocampal cultures. For analysis of spine user need to select a dendritic segment by marking the two points and then automatically segment the spines using the designed convolution kernels and finally mark the spines of interest to extract relevant features like length and head width of spine with high accuracy and minimal intervention. This method counts number of dendritic spike along with the classification of four types of segmented dendritic spine (Stubby, Mushroom, Filopodia and Spine-head Protrusion). This method allowed to record noticeable changes in area and length of dendritic spines which are the two most important attributes for spine plasticity. 2dSpAn requires considerably less user involvement in comparison to the work by Ruszczycki et al., [24]. As a result, large number of spines can be annotated quickly and effortlessly without compromising on the accuracy of the estimated spine features. This work completely depends on the selection of the interested dendritic region by user. Then

a global binarization is performed over the image which sometime causes to a noisy result and improper segments of interested spines.

Dr. T. Worbs *et al.,* [25] developed Imaris software for four dimensional (4D) image analysis and automatic neuron tracing. Using Imaris for Neuroscientists users can manage and organize full experiments including images and data analysis. Advantage of Imaris is high performance IMS file format which guarantees smooth navigation even in very large 3D datasets (TB range). The accuracy of the automated tracking was manually controlled, and only tracks with durations of >60 s was included in the analysis. Although Imaris is good for analysis overall spine analyzing but due to huge manual intervention it fails to model the 3D morphology of individual spine.

Swanger *et al.,* [26] also proposed an automated method for analysis of dendritic spine morphology in 4D. They used Imaris suppress mode to find the region of interest. But user need to assign dendrite starting point manually

Pheng Shi *et al.,* [27] proposed a novel semi-supervised learning (SSL) approach to determine morphological classification of dendritic spines online. In their approach dendritic spines are detected and segmented from dendrite based on wavelet transform. Then spine features are extracted and SSL is applied. But the overall performance of this method is dependent on the features and segment selected by the neuro-biologist for training.

An algorithm for 3D reconstruction and identification of dendritic spine was proposed by Janoos *et al.,* [28]. This is based on skeletonization approach. Firstly, the find the skeleton of the whole dendritic spine and then the longest centre line is considered as dendrite and the smaller ones are considered as spine. Although this approach robustly reconstructs dendritic spines in 3D but the time required to get the centre lines (skeleton) from 3D volume and complex image is very expensive.

Rodriguez *et al.,* [29] proposed a 3D neuron analysis approach based on 3D reconstruction using Ray burst diameter. The Rayburst diameter in each layer of a spine was calculated and the head and neck of each spine was defined according to the distribution of the diameters. This method detects and classify the spines in an efficient way but there are certain probabilities to fail to segment correctly in case of very complex structure of spine and the classification has been done based on the Head-Neck Ratio. But the global threshold for the Head-Neck ratio is not adaptive so for analysis of different kind of image may efficiency may vary.

In 2018 Basu *et al.,* [30] [31] proposed a method for quantitative analysis of individual dendritic spine in 3D. They use three-dimensional segmentation of spines using Multi Scale Opening (MSO) [31] approach to determine the 3D morphometric features of individual spines for quantitative analysis of spine plasticity. They were using confocal light microscopy images of dendritic spines from dissociated hippocampal cultures and brain slices. Although their method did not calculate the spine density as it require more time but still produce a good result.

Therefore, still there is a scope to improve the performance of this tool especially in the context of a better user interface and some pre-processing steps.

CHAPTER 3

SURVEY OF DIFFERENT IMAGE REGISTRATION TECHNIQUES

Medical Imaging diagnostics undoubtedly has become a major area of research over the past few decades and has consequently revolutionized the way in which modern medicine is practiced. There has been a great enhancement in the design of algorithms at a very fast pace and these algorithms are assisting medical physicians in diagnosing patients. In many cases, it is of great significance to separate out key regions of the image to obtain data for adequate analysis. The alignment of images spatially is the first step to obtain such information. This process is known as image registration. Image registration is a process which aligns two or more images of the same scene. Spatially mapping the coordinate system of one image to the coordinate system of another image is the main idea behind image registration. Images can be misaligned for a variety of reasons. Commonly, images are captured under variable conditions that might the camera perspective or the scene's contents. Misalignment can also result from lens and sensor distortions or differences between capture devices. Image registration techniques can be classified into two main categories: rigid and non-rigid image registration techniques. Rigid registration takes into consideration basically is a global transformation and the transformation will be based on certain parameters tuning which can change the differences between two or more images. Non-rigid registration on the other hand takes into consideration any local deformation that might occur due to cases like tissue movement, for example. Image registration can sometimes be a bit too computationally expensive but the general idea behind it is relatively simple and intuitive. The algorithm can be stated as follows:

- Suppose we are given 2 images to be registered we need to designate one of them as the reference image and the other one should denote the mis-registered floating image. The goal is to find appropriate transformation for the floating image until it bears close resemblance with the reference image.
- We need to choose a criterion that will quantify the match/mismatch between the reference and the transformed floating image. Also a stopping criterion needs to be chosen indicating that the images have been registered.
- Optimize the transformation on the test image such that the stopping criterion is met.

The choice of criterion function is the core of the registration process. Comparison methods such as cross-correlation and mutual information are some of the more common techniques

found in the literature [47]. Since its introduction in 1995 by Viola and Wells [49], mutual information has been one of the most discussed and (usually) acclaimed registration measures for multi-modal image registration [48].

The field of image registration is an immensely ever expanding field. By the early stages of 1993 it has been estimated that over 120 papers existed on the registration problem, as cited in a comprehensive survey article written by van dan Elsen et al. [32] Since then the number of papers published have grown exponentially. This technical report is focused on presenting the user with a thorough literature review on general image registration techniques especially how they are classified. Additionally 2 cutting edge image registration algorithms that have been used in the method will be discussed and analyzed completely.

3.1 DIMENSIONALITY – 2D, 3D, 4Ds

It is quite evident we can classify the image registration techniques based on the number of dimensions used. This can range from a simple 2D registration process right up to a complex time series registration of 3D data, i.e. a 4D process. The issues regarding the dimensionality of registration algorithms shall be grouped into those that do not deal with time series registration and those that do. Algorithms not dealing with time series registration are the ones.

3.1.1 REGISTRATION IN SPATIAL DIMENSIONS

From the algorithms dealing with spatial dimensions, a further classification may be made, i.e. 2D, 3D. 3D registration is a trending area of research which is considerably complex than 2D registration. 2D registration is also very important in the medical imaging domain. The direct use being registering 2D images which is a relatively simpler task compared to 3D registration because of the reduced data size and also because of the reduced parameter set which is used in the registration process. Another important application of 2D algorithms is the process of reconstruction. This is the process of generating a 3D image from a series of 2D slices. Before the stacking of 2D slices happen, it is important that each slice be registered with its neighboring slices if the resulting 3D image is to maintain close resemblance with the same anatomical region that it was originally scanned from. Another definable area of the dimensionality criteria is in the registration of 2D to 3D images. An example of this is the registration of 3D tomographic data to a 2D projection image such as an X-ray. This process is often employed during surgical intervention, i.e. intra-operative procedures. It is of paramount importance to note that any registration algorithm that is involved in intra-operative procedures must be extremely efficient and fast in order to be

carried out in real time during the period of intervention. However, most other applications that involve registration can be done outside the surgical theatre allowing for less stringent time constraints on the computation time required to complete the registration process. Thus, it is the clinical relevance of the required registration algorithms that should set constraints on speed issues.

3.1.2 REGISTRATION OF TIME SERIES

Another area where image registration algorithms are in application is to a set of images acquired over time, i.e. time series registration. Such a procedure gives medical practitioners the ability to monitor numerous different situations which may arise during a patient's life. Perhaps the most obvious application is in the study of the evolution of a tumor, during which images are acquired over a period of time (days, weeks, months, and years) and are inspected to determine factors such as the rate of growth. Other applications of time series registration is in the monitoring of bone growth (usually in children). This process takes quite a long time. Also, the monitoring of a patient's healing after a surgical intervention or some other form of medical procedure such as radiotherapy is another extremely important application of time series registration. This usually occurs over a much shorter interval. Other applications include the monitoring and evaluation of the effect of certain drugs.

3.2 NATURE OF THE REGISTRATION ALGORITHM

The nature of the registration algorithm is an expression that is used to describe the method of the registration algorithm in terms of what characteristics or features are matched between images. This is an area in which registration algorithms are dissimilar. The main distinction that can be made is between those that use extrinsic or intrinsic methods.

3.2.1 EXTRINSIC METHODS

The first variety of registration algorithms that were developed employed the use of extrinsic methods. These techniques introduce alien objects into the imaging space by attaching them in some way to the patient before imaging. These foreign objects are called fiducial markers, are designed in such a way so that they appear visually in the resulting images acquired after scanning. These fiducial markers should be such that they are easily distinguishable from any other region in the image. The main motive behind using these extrinsic markers is that these easily distinguishable features may be then used in the registration process.

Perhaps the most well-known form of fiducial marker is the stereotactic frame. This is a device which is screwed into the patient's skull before imaging and until recently, registration methods employing the use of a stereotactic frame were deemed as the 'gold standard'. [33] A stereotactic frame is also heavily used in neurosurgery for guidance purposes and also in other stereotactic procedures – a blind surgical procedure whereby the target is approached from a small twist-drill hole in the patient's skull [34]. There are also other invasive markers that can be used including screw mounted markers.

As extrinsic methods have been designed with the registration process in mind, they are quite accurate and also remarkably fast. This is due to the fact that it is known when the images are registered as the corresponding fiducial markers will be appropriately aligned. This is due to the fact that it is known when the images are registered as the corresponding fiducial markers will be appropriately aligned. This eliminates the need for any elaborate optimization algorithms that generally slow down the optimization procedure dramatically. Also, extrinsic methods are often related to only rigid transformations since, by definition, extrinsic methods cannot include any patient related information. However, the disadvantages of extrinsic methods includes their perspective nature, i.e. steps must be made prior to the imaging process, and their invasive nature with respect to patient comfort.

3.2.2 INTRINSIC METHODS

Intrinsic methods offer an enormous area of exploration for the solution of the registration problem. These methods are based solely on the information which is contained in the patient's scan and does not rely on the introduction of any artificial objects into the imaging process. Intrinsic methods range from simple points that correspond to an anatomical landmark to complex 3D structures that are used in the matching process. More specifically, intrinsic methods are subcategorized into the following:

- **Anatomical Landmarks:** The first form of intrinsic based registration used anatomical landmarks as the matching feature between images. Anatomical landmarks are points within the images that can be identified by a user and which correspond to some distinguishable point within the morphology of the anatomical image. Technically the identification of anatomical landmarks is a manual segmentation process. However, the segmentation based methods are reserved to those that use much more complicated means to segment higher order structures and/or processes that are solely implemented by computational means.

- **Segmentation Based:** Segmentation based methods offer an enormous and comprehensive range of possibilities for solving the registration problem. They are labelled with this name as a segmentation or other feature extraction procedure must be executed in order to obtain required features for matching. This segmentation can be a user guided or automatic computational procedure. The resulting features utilized include geometrical points, curves and surfaces. Geometrical points like anatomical landmarks are point features obtained from an image. These are the lower order segmentation methods available and are usually extracted in automatic fashion. These type of features are generally referred to as geometrical landmarks as they can be considered stable points within the image, i.e. landmarks, which can be reliably used in the matching process. Although these type of points can be considered analogous to anatomical landmarks but they are different considering the fact that computational processes must be undertaken in order to extract points. These points are usually generated using some means of differential geometry and, like anatomical landmarks are generally only used for rigid registration processes.

- **Intensity Based:** Intensity based registration methods also referred to as voxel property based methods, are significantly different from segmentation based registration methods. These methods operate directly on the intensity (or grey level) values within the image and thus do not need to utilize complex segmentation procedures or other feature extraction methods in order to obtain features required for matching. These methods are generally the most flexible and robust of all registration methods as they make no assumptions on the underlying information contained within an image. There are also numerous ways in which the image data may be utilized in the registration process [35]. However they can be quite computationally expensive as they operate on the full image content rather than a respective structure such as a surface. The first form of intensity based methods were known as principal axes or moment base methods. These methods operate by first reducing the entire image data into a set of vectors. This is accomplished by the extraction of the zeroth and first order moments (or sometimes higher) from within the image. The registration process then lies in a transformation that will match the image's centers of gravities and overlay their respective principal directions. Another significant group of intensity methods are those that are based on correlation. These methods were introduced to help overcome the problem of the differing levels of intensity between the images. This was accomplished by assuming that there existed some linear correlation between the intensity values of two images. Perhaps the most promising intensity-based approach for improvement of multi-modal registration

techniques is mutual information [36]. This measure is based on the entropy of image intensities and derives its origins from information theory. It can be used to compute an optimal registration by adjusting the relative position and orientation of the images until the mutual information between the two is maximized. This technique provides a more flexible and robust approach compared to most other intensity-based techniques and is rapidly finding itself being used in more and more clinical applications.

3.3 NATURE & DOMAIN OF TRANSFORMATION

The criteria of the classification deals with the nature and domain of the transformation that is employed by certain registration algorithms.

3.3.1 NATURE OF THE TRANSFORMATION

Registration techniques are often grouped into two very general categories namely rigid and non-rigid registration. This is known as the nature of the transformation. This classification is however not adequate to sufficiently describe the differences which may exist between various registration algorithms. A more specific approach is to classify registration algorithms into the following categories.

- **Rigid**
- **Affine**
- **Projective**
- **Curved**

A rigid transformation is the most fundamental of all registration techniques. Such a transformation involves only rotation and translation in order to bring the images into alignment. An affine transformation incorporates a shearing into the rigid registration process. This effectively maps parallel lines onto parallel lines. A scaling factor is also often incorporated into an affine transformation. A projective transformation is one in which any straight line is mapped onto another straight line. These lines however, may not be necessarily parallel. The final transformation is a curved transformation. This is one way in which any straight line is mapped onto a curve. A curve transformation is also often referred to as an elastic transformation.

As you descend the transformations listed above, the mathematical and thus the computational complexity of the transformation increases dramatically. This concept can

be seen in the implementation of certain registration algorithms in clinical applications. Often registration algorithms are employed in real-time surgical interventions for instance to register intra-operative images to pre-operative images acquired earlier. However, it is often rare (yet becoming prevalent), to find an elastic based registration that is involved in a real-time application.

3.3.2 DOMAIN OF THE TRANSFORMATION

The domain of the transformation deals with the concepts of local or global transformations. Before explaining this any further the notion of a transformation must be first understood. A transformation can be defined as a mapping of points in one image to a new set of points in other image. However, this mapping can be applied to the image locally or globally. A global transformation is the case when the entire image is mapped in the same way, i.e. a single equation can be given which maps the entire image. A local transformation is the case when the image is mapped in a different way depending on the spatial location. Thus, local transformations are much more complex procedure and are much harder to express concisely.

3.3.3 RELATED ISSUES OF TRANSFORMATION

Global rigid transformations are by far the most utilized registration techniques seen throughout the literature and in clinical applications. This is due to the concept of rigid body constraint that can be successfully applied to many situations in the registration field. The rigid body constraint is a simple assumption made regarding the object being registered, which assumes that the object is a rigid body i.e. nothing internal may move. This assumption is valid for a large number of registrations involving the head.

Most multimodal registrations, for example, assume the rigid-body constraint. Intra-subject registration also generally makes this assumption. Although the brain may move internally between successive acquisitions of the same patient, this assumption is still usually valid as a good approximation. However, for inter-subject registration, registration with an atlas, and registration with other parts of the body (for example the abdomen), the rigid-body constraint is no longer adequate.

3.4 INTERACTION

This criteria of the classification deals with the amount of interaction that is required by the user of the registration algorithm. Within this criteria, three subcategories can be defined. These are listed below.

- **Interactive**
- **Semi-Automatic**
- **Automatic**

Traditional manual methods whereby a trained physician visually found a spatial mapping between two images can be classified into the interactive category. With any interactive methods the user generally does all the work manually with some help from a software based platform that displays the current state of registration to the user. Interactive methods may also often supply an initial guess for the registration required. It is then left to the discretion of the user whether or not this guess is used. Fully interactive systems are seldom used in the literature. This is due to the inherent subjectivity which is introduced into the registration process by the interaction with the humans. Also, these methods rely heavily on adequate (and often very expensive) visualization software to display and provide controls to manually manipulate images.

Semi-automatic methods are quite popular especially in clinical applications as they will allow some control inputs from the user. This is often a good idea in applications where the result of the registration process can have profound effects on the end result. Thus, the attending physician generally desires to oversee the registration process in order to make sure it has aligned and converged properly [37].

Fully automatic methods are the most objective methods currently available as they require no control inputs or initializations to be entered by the user. In a fully automatic system, the user generally only supplies the images that need to be registered and maybe some other parameters which define certain characteristics such as what imaging modalities the input images were acquired from. It is these type of registration approaches that are currently experiencing a rapid serge in research. As briefly mentioned above most of the current research is directed towards the development of fully automated registration systems. However, not all clinical systems necessarily benefit from this approach. There generally exists form of trade-off relationship between the user interaction, the resulting speed of the registration process and other design criteria such as the robustness.

3.5 OPTIMIZATION PROCEDURES

There are certain optimization procedures that are employed by registration algorithms in order to compute the required transformation procedures. The parameters that are obtained are then used to drive the registration process. A global rigid transformation only requires six parameters to describe the transformation. However, an elastic or fluid registration will typically have hundreds, thousands or even millions of parameters. The two main distinctions that can be made between registration optimization procedures are listed below.

- **Direct methods**
- **Approximation or search-oriented methods**

A direct method obtains the transformation parameters directly from the available information. However, approximation methods search for the transformation parameters based on some form of optimization of a function defined in the parameter space.

The computation method for the direct approach solely depends on the nature of the registration algorithm. Generally, global transformations that compute the required parameters directly only involve small amounts of information, i.e. only a small set of features are used in the process such as sets of corresponding points. As the number of points increases so too does the accuracy of the registration. Local transformations can often be computed directly from the local information available in the image and does not require a set of features to be pre-defined. Optimization procedures that search for the transformation parameters generally accomplish this by formulating the registration model in a mathematical equation that incorporates the transformation parameters. The transformation parameters are then computed in order to optimize the defined function in some sense. An example might be to find the transformation parameters that minimize a certain distance metric which is computed between the two images. It may also involve the maximization of a similarity criteria such as the correlation or mutual information between the images. If the optimization procedure employed in the registration is well behaved, i.e. optimization function forms a quasi-convex shape, then any of the numerous standard and well researched optimization techniques can be employed. Some examples of optimization methods are listed below.

- **Powell's method**
- **The renowned Newton-Raphson iteration method**
- **The downhill simplex method**
- **Gradient Descent methods**
- **Genetic methods**

If the optimization function used by the registration process is not well behaved, then the only technique that allows transformation to be computed is an exhaustive search of the entire parameter space. Such a method involves extreme amount of computational time due to the lengthy process of applying each value for each registration parameter in essentially a trial and error basis. Thus, exhaustive searches are not very practical methods.

3.6 SKELETONIZATION

Skeletonization is a process in which the foreground regions from a binary image are reduced to a skeletal remnant. It largely preserves the extent and connectivity of the original region of interest while removing most of the foreground pixels. Skeletons are effective shape abstractions used in segmentation, shape matching, reconstruction, virtual navigation, etc [53]. The skeletonization algorithm used requires a binary image as input and output is the thinned skeleton which is also a binary image. The figure 3.1(a) shows the image input image of a horse and figure 3.1(b) shows its skeleton.

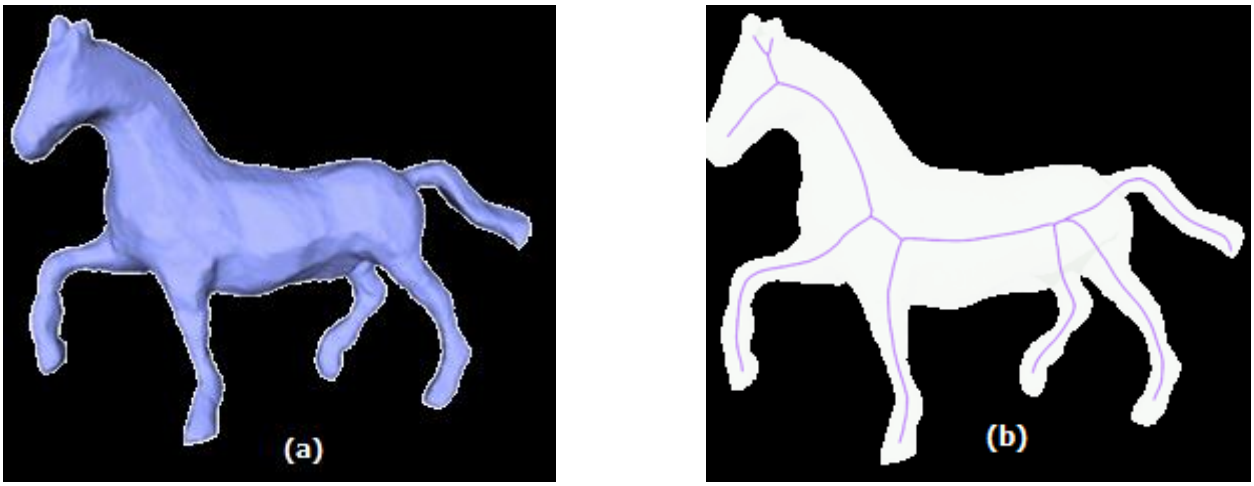

Fig 3.1 Image representing shape of a horse (a) Original Image (b) Skeletal Shape of the horse

Ideally the skeleton should be re-constructible which implies that it should be possible to construct the original image from the skeleton. A skeleton should intuitively maintain the topological properties, i.e. to retain the topology of the original object. The skeleton should also preserve the geometrical properties, i.e. the skeleton should be constrained to be In the middle of the object and invariant under translation, rotation and scaling. To see the working mechanism, imagine that the foreground regions in the input binary image are made of some uniform slow-burning material. Light fires simultaneously at all points along

the boundary of this region and watch the fire move into the interior. At points where the fire traveling from two different boundaries meets itself, the fire will extinguish itself and the points at which this happens form the so called `quench line'. This line is the skeleton. Analytically Skeletonization [38] can be defined as a grassfire transform where we think of the object to be a field of dry grass that is simultaneously lit at all boundary points. The fire burns the grass-field at a uniform speed and the set of quench points, where two independent fire fronts actually collide, forms the skeleton of the object. The centers of maximal balls (CMB) are used to define quench [39] [40] points which form the skeleton. The figure 3.2(a) shows the input image of a dendritic spine and figure 3.2(b) shows its skeleton.

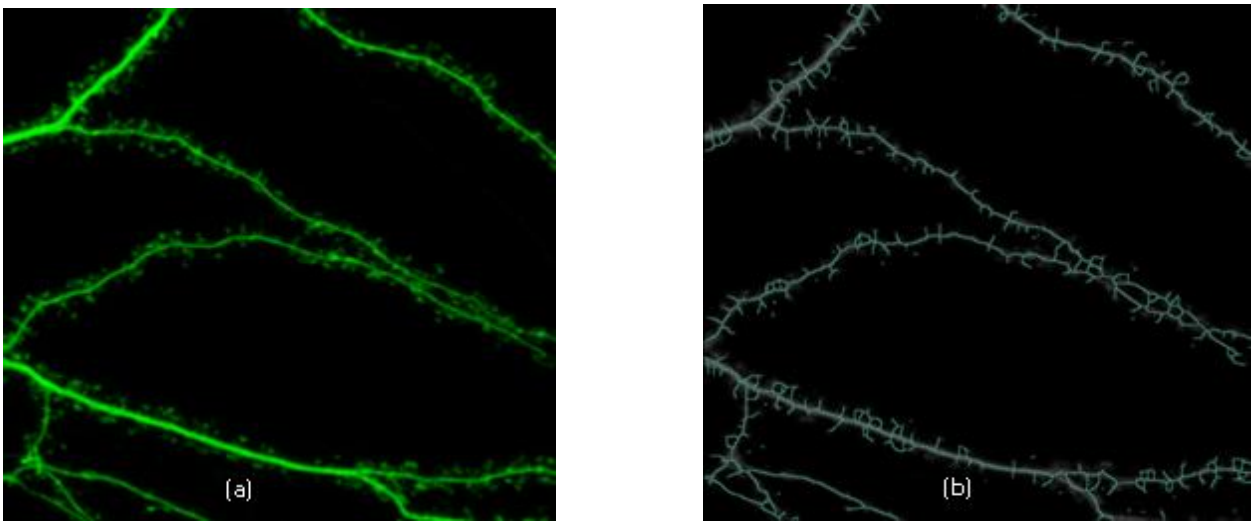

Fig 3.2 Image of dendritic spine after chemically induced long term potentiation (cLTP) (a) Original Image (b) Skeleton of the image

Skeletonization has found its applications in many image processing and computer vision applications including object representation, retrieval, manipulation, matching, registration, tracking, recognition, compression, etc. The compactness feature of skeletons facilitates efficient assessment of local structural metrics including scale, orientation, topology, geometry, etc. This specific feature of skeletons has been explored for quantitative characterization object morphology in several imaging applications. Skeletonization has been used in various medical imaging areas including pulmonary, abdominal, retinal, bone imaging, cardiac, mammographic, etc.

In our method we apply Distance Transform (DT) based skeletonization followed by the concept of center of maximal balls, collision impact (CI), simple point, etc. The major steps used in our skeletonization method is as follows:

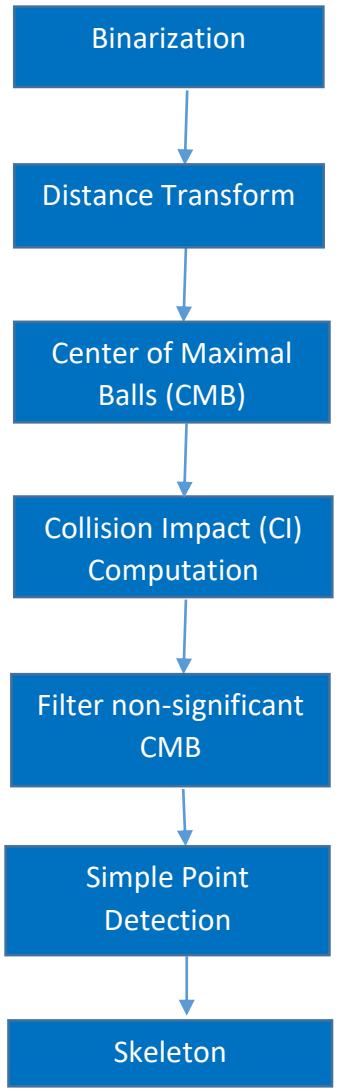

Fig 3.3 The major steps in to obtain the skeleton

The first step in Skeletonization is to binarize the input grayscale image. Binarization converts the grayscale image which consists of values in the range (0-255) to a binary image which can have only 2 possible values (0 or 1). Typically, the two colors used for a binary image are black and white. Binary images are also called *bi-level* or *two-level*. This means that each pixel is stored as a single bit—i.e., a 0 or 1. Binary images are used for simplification of the image and are used to represent basic shapes and line drawings. In case of medical images the binarized image obtained is not of great quality due to poor image acquisition schemes. Varying regions of intensity are seen in images of objects like arteries, veins, etc. which makes obtaining a high quality binary image very difficult. So, it becomes

a very important step to choose a binarization method that inhibits non-feature pixels from becoming a part of the subject for processing and potential cause of errors for post-processing steps. The advantage of obtaining a binary image is that it reduces the complexity of the data and simplifies the process of recognition and classification.

The most common way to convert a gray-level image into a binary image into a binary image is to select a single threshold value (T). Then all the gray values below T will be classified as black (0) i.e. background and those above T will be white (1) i.e. objects.

$$g(x, y) = 0 \quad \text{if } f(x, y) < T$$
$$= 1 \quad \text{if } f(x, y) >= T$$

(x, y) are the co-ordinates of the pixel under consideration. 'T' represents the threshold value, f(x, y) gives the intensity of the input gray-level image at point (x, y) and g(x, y) represents the pixel value at (x, y) after applying threshold 'T'.

In this work Otsu's method of binarization has been used. In global thresholding generally we use an arbitrary chosen value as a threshold. In contrast Otsu's method avoids having to choose a value and determines it automatically. Consider an image with only two distinct intensity values (bimodal image) where the histogram would consist of only 2 peaks. A good threshold will be in the middle of those two values. Similarly, Otsu's method determines an optimal global threshold value from the image histogram. In the proposed method the image is first filtered with a 5x5 gaussian kernel to remove the noise then Otsu's thresholding is applied directly. The figure 3.4 shows histogram of a bimodal image. For that image, we can approximately take a value in the middle of those peaks as threshold value.

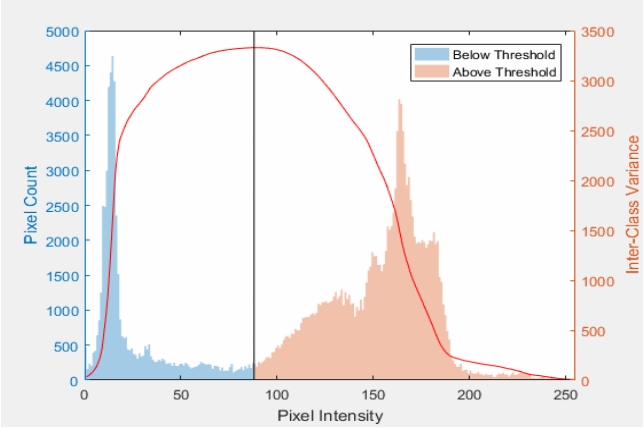

Fig 3.4 By Lucas(CA) - Own work, CC BY-SA 4.0, https://commons.wikimedia.org/w/index.php?curid=67144384

Next we need to calculate distance transform (DT) of the image which is an operation that converts a binary picture, consisting of feature and non-feature elements, to a picture where each object pixel gets a value that is equal to the distance between itself and the nearest point in the background i.e. Distance into a shape. Each background pixel gets a value that is equal to the distance between itself and the nearest point in an object i.e. Distance from a shape. Therefore, in the resultant image each element has a value that approximates the distance to the nearest feature element. The figure 3.5(a) shows the concept of distance into a shape and figure 3.5(b) distance from a shape.

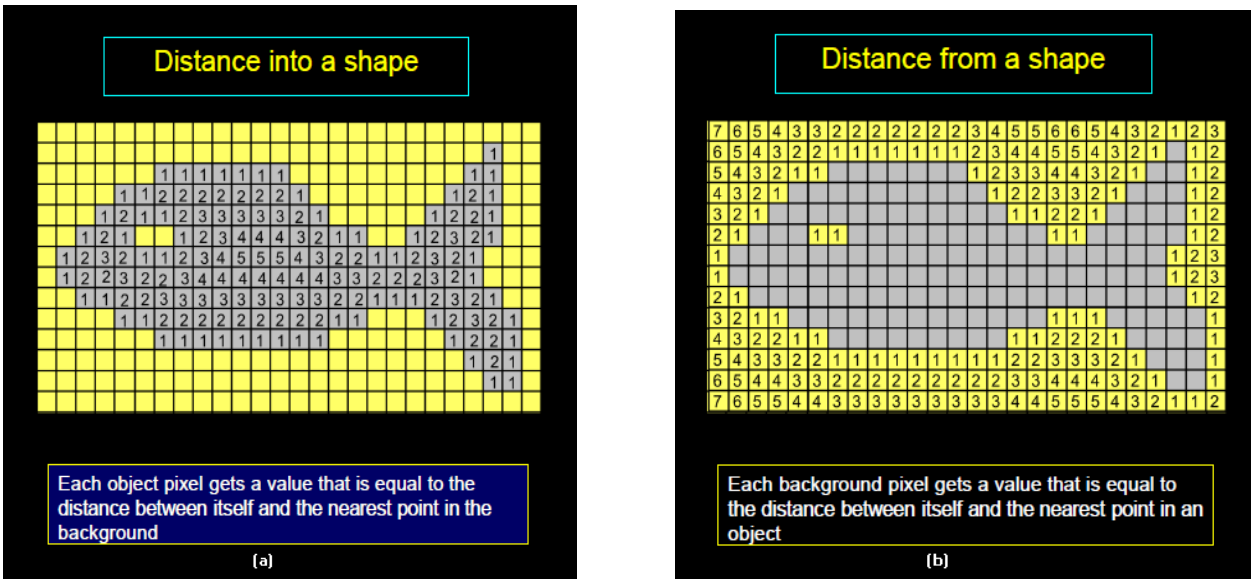

Fig 3.5 Distance Transform in a fish-shaped figure (a) Distance into a shape (b) Distance from a shape

There are different DT methods proposed so far. The most popular one is the city block/chessboard distance family, here called n-neighbor distance [41]. City block distance d_4 can be mathematically expressed as,

$$d_4((x_1, y_1), (x_2, y_2)) = |x_1 - x_2| + |y_1 - y_2|$$

Chess board distance d_8 can be mathematically expressed as,

$$d_8((x_1, y_1), (x_2, y_2)) = max(|x_1 - x_2|, |y_1 - y_2|)$$

To compute the chess board distance two masks shown in figure 3.6(a) and 3.6(b) are passed over the image one at once. The forward pass is started from left to right and from top to

bottom and the backward pass is stared from right to left and from bottom to top. The new value of the central pixel is the minimum of the sum of the local pixel values and distance d1 or d2. For figure 3.6(c) values of d1 and d2 are assumed to be 1 and 2 respectively. Distance is propagated from a single centre point numbered as 0. If we connect the equidistant points, it will take the diamond like shape (figure 3.6(e)) that is why city block is also called diamond distance.

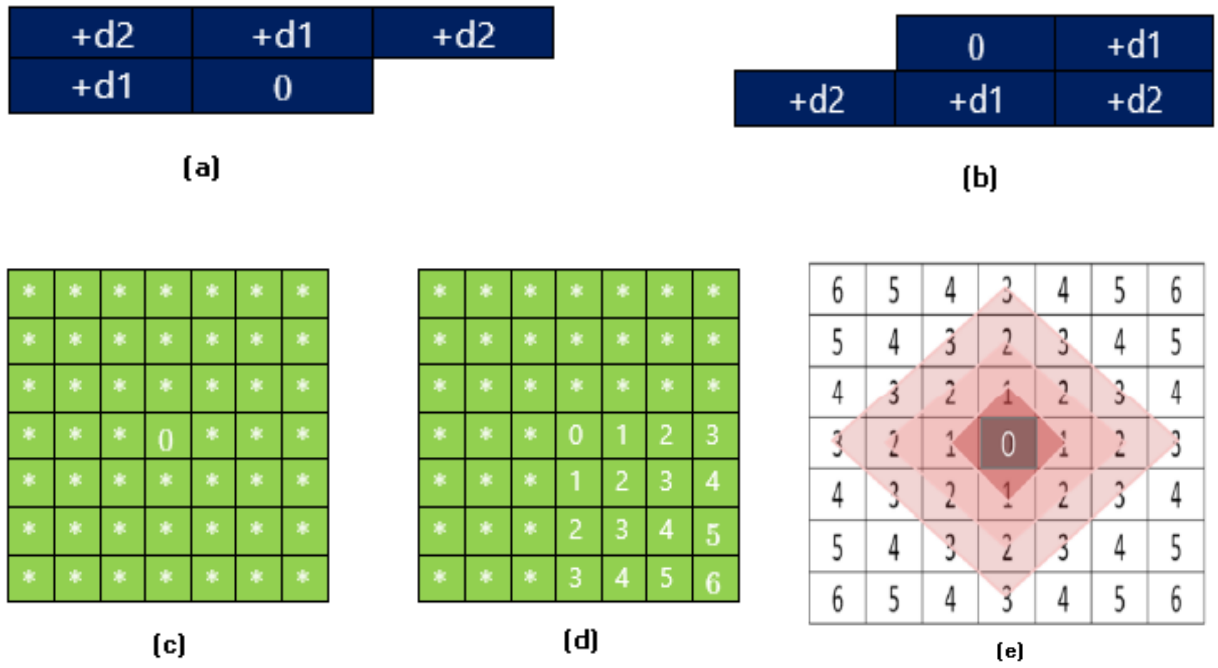

Fig 3.6 Mask & computation related to chessboard distance (a) Forward mask (b) Backward mask (c) Original image (d) Image after forward pass (e) Image after backward pass

DT is widely applied in many applications including centre of maximal balls, Voronoi neighborhood, DT-based interpolation, multi-scale opening of conjoined structures and quantitative assessment of object morphology. In our method we apply DT as a pre-processing step to skeletonization. Applications are digital image processing (e.g., blurring effects, skeletonizing), motion planning in robotics, and even path finding. The distance transform can also be used for font rendering using vectors instead of sampling from texture.

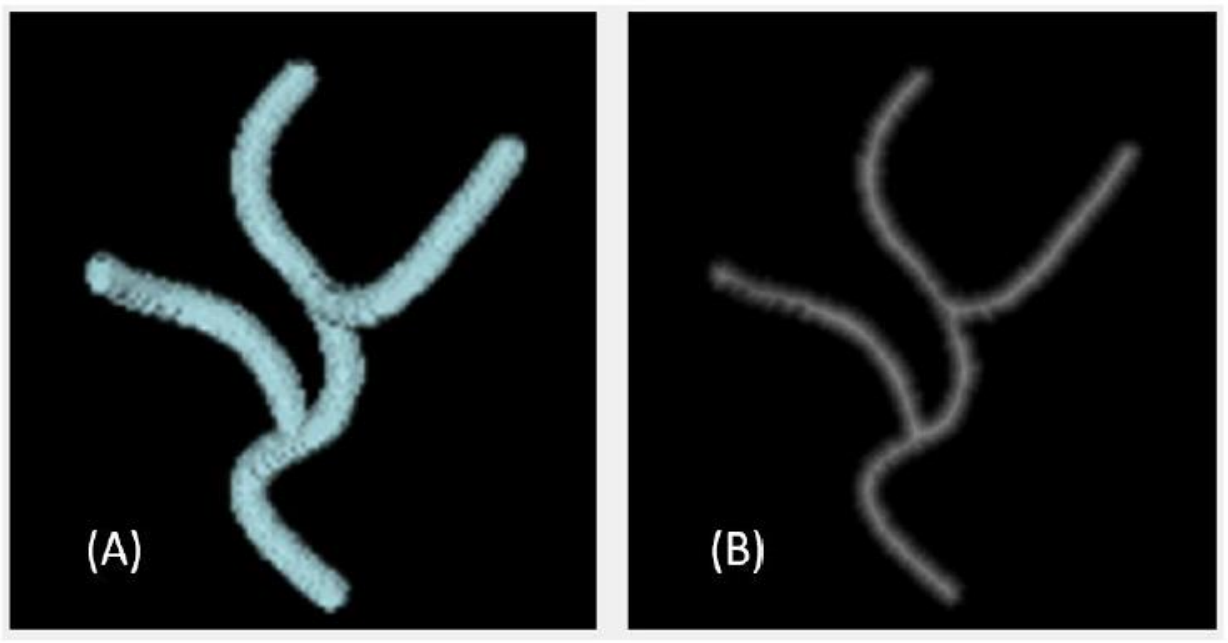

Fig 3.7 Mathematically generated phantom of bifurcation (a) Original image (b) Image after applying Distance Transform (DT)

The next step is centre of maximum ball (CMB) calculation. Centre of maximum ball (in 3D) or disk (in 2D) is maximal if it fills the object inside which it is placed fully and there is no other point that can be placed inside the object that can cover it at that point. The skeleton of an object is defined as the loci of the centres of maximal included disks.

Idea:

- To place all possible maximal disks inside the object and finding their centres.
- The Skeleton of the object is a set of all such centres of possible maximal disks.

Let **B** is the structuring element that represents the maximal disks.

- Then 0B represents the origin of the maximal disk.
- Then B, 2B, 3B…..nB represents all possible maximal disk.

– Let skel(S) be the set of all centres of the maximal disks.

$$Skel(S) = (A \ominus nB) - [(A \ominus nB) \circ B]$$

– So, the Skeleton(S) of the object is

$$(S) = \cup Skel(S)$$

Where, A Θ nB represents successive erosions of the image A by the B and $A \Theta B = \bigcap_{b \in B}^{n} A_b$.

The figure 3.7 shows the concept of centre of maximum ball.

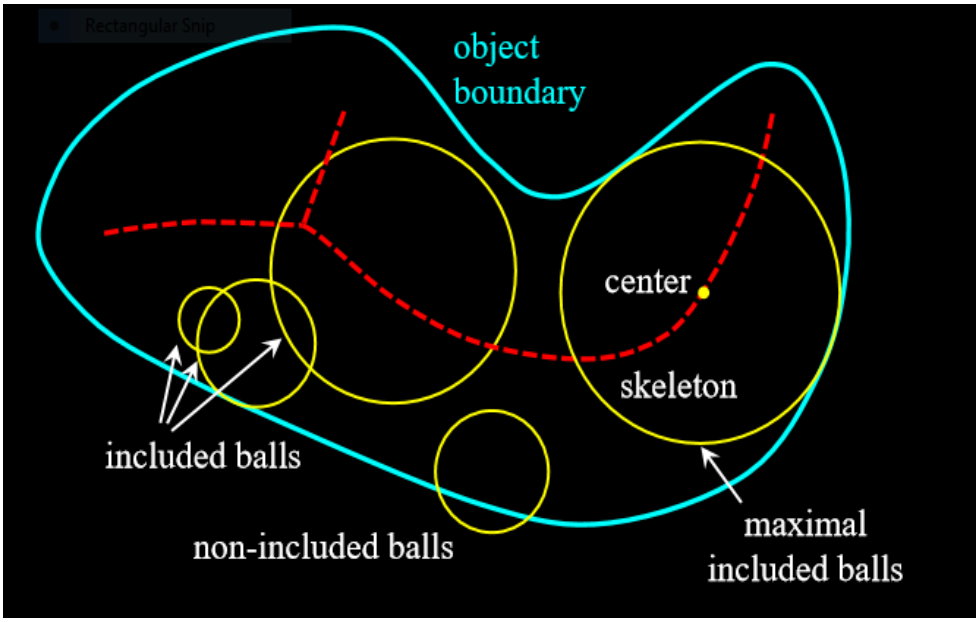

Fig 3.8 Centre of Maximum Ball/Disk

The next step is collision impact calculation. The quench points, defined as the locations of colliding fire-fronts, have been well explored in the context of skeletonization in the form of CMBs. In grassfire transformation two colliding fire-fronts stops at quench points but their collision impact may vary depending on the angle between them. The natural speed of fire-front propagation is interrupted by the colliding impulse of fire-front coming from the opposite direction. Here, collision impact for pixel P for every Q∈ N_8 (P) is defined as

$$CI(P) = 1 - \underset{Q \in N_8(P)}{MAX} \frac{dt(Q) - dt(P)}{|P - Q|}$$

Now, we need to filter the non-significant CMB points while retaining the significant one. Thus, we delete the unwanted branches of skeleton.

Next we need to delete the simple points. Simple points of an object are those points whose deletion does not affect the topological and geometrical properties of the object. A point P is a 2D simple points if it satisfies the following conditions:

- P has 4-background neighbor
- P has 8 object neighbor
- The set of 4 background-neighbor of P are connected.
- The set of 8 background-neighbor of P are connected.

The figure 3.8 shows the simple points in blue and critical points in green.

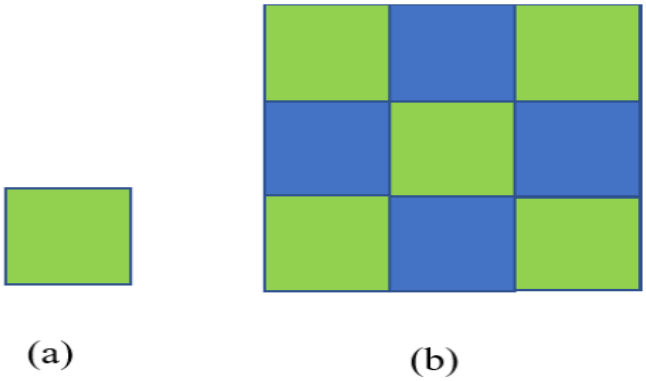

Fig 3.9 Simple Points

3.7 IMAGE REGISTRATION TECHNIQUE

Registration is a general term that is used to describe the process of developing a spatial mapping between sets of data. Such a procedure can find applications in many diverse fields within the research community including engineering, science, medicine, computer vision, robotics and image processing. Within these major fields, registration has specific applications in areas such as stereo vision, remote sensing, image stabilization, reverse engineering and automated manufacturing, satellite navigation, photogrammetry, video/image compression and coding, pattern recognition, tracking, video microscopy and of course medical imaging. More specifically the objective of registration is to match two or more images maybe that are acquired at a different time from different sensors or from different viewpoints [42]. However, due to the immense complexity of the human anatomy, medical image registration turned out to be a much more difficult process than originally expected. Registration plays a crucial role in the medical imaging field where continuous advances in imaging modalities including MRI, CTI and PET allow the generation of 3D images that explicitly outline detailed in vivo information of not only human anatomy but also human function. A common task within the medical imaging field is the fusion of

complimentary and synergistic information provided by the various imaging modalities. This process is known as multi-modal registration. Another common task is the registration of images of the same patient taken at different times and/or in different positions. This process is referred to as mono-modal registration and can be used to track any pathological evolution. Other applications include inter-patient registration and patient atlas matching. The first two applications are generally solved with rigid registrations, i.e. only rotations and translations are used in the transformation. However, last two examples are generally performed with a non-rigid registration. This allows one image to be deformed to match another in order to account for the non-linear local anatomic variations that exist between the images.

3.7.1 MUTUAL INFORMATION SIGNIFICANCE IN RIGID BODY REGISTRATION

Mutual information is a technique that has been successfully used as a comparison function for registering images. It is a measure of how much information one image contains about another. In this work, mutual information has been used as an objective function for finding the best transformation that will align the misregistered image with the original image. This work is restricted to rigid affine transforms only (e.g. rotation, translation, scaling and skew). The parameters yielding the maximum mutual information will be the parameters that best register the misregistered image. Since its introduction in the year 1995 by Viola and Wells [43] mutual information has been one of the most discussed and (usually) acclaimed registration measures for multi-modal image registration [44]. Mutual information is a statistical measure that assesses the strength of dependence between two stochastic variables. Even though mutual information has been shown to outperform other comparison methods used for registration, it is not a panacea [15]. The process can often be improved by incorporating spatial information when performing the alignment [45]. In this work main focus is to describe how mutual information can be used to perform rigid-body registration. Mutual information (MI) is a statistical measure that finds its roots in information theory. MI is a measure of how much information one random variable contains about another. The MI of two random variables A and B can be defined as:

$$I(A,B) = \sum_{a,b} p_{A,B}(a,b) \log \frac{p_{A,B}(a,b)}{p_A(a) \cdot p_B(b)} \qquad (3.1)$$

$p_{A,B}$ (a, b) is the joint probability mass function (pmf) of the random variables A and B, and p_A(a) and p_B(b) are the marginal probability mass functions of A and B respectively. In working with images, the functional form of the pmf is not readily accessible. The

normalized histograms of the intensity values for each image serves as a good approximation of the pmf. The MI can also be written in terms of the marginal and joint entropy of the random variables A and B as follows:

$$I(A,B) = H(A) + H(B) - H(A,B) \tag{3.2}$$

H (A) and H (B) are the entropies of A and B respectively and H (A, B) is the joint entropy between the two random variables. They are defined as follows:

$$H(A) = -\sum_{a} p_A(a) \log p_A(a) \tag{3.3}$$

$$H(A,B) = -\sum_{a,b} p_{A,B}(a,b) \log p_{A,B}(a,b) \tag{3.4}$$

One interpretation of entropy is as a measure of uncertainty of a random variable. A distribution with only a few large probabilities has a low entropy value; the maximum entropy value over a finite interval is achieved by a uniform distribution over that interval. The entropy of an image indicates how difficult it is to predict the gray value of an arbitrary point in the image. MI is bounded by cases of either complete dependence or complete independence of A and B, yielding values of I = H and I = 0 respectively where H is the entropy of A or B.

The strength of the mutual information similarity measure lies in the fact that no assumptions are made regarding the nature of the relationship between the image intensities in both modalities, except that such a relationship exists. For image registration, the assumption is that maximization of the MI is equivalent to correctly registering the images. It is clear in Eq. 3.2 that if the joint entropy of A and B are not affected by the transformation parameters, maximizing the MI is equivalent to minimizing the joint entropy. The joint entropy is minimized when the joint pmf of A and B contain few sharp peaks. This occurs when the images are correctly aligned. When the images are misregistered, however, new combinations of intensity values from A and B will cause dispersion in the distribution. This dispersion leads to a higher joint entropy value, which in turn decreases the MI.

3.7.2 RIGID BODY IMAGE REGISTRATION

As the name suggests in rigid body transformation the object remains 'rigid' we don't alter the geometry of the object, just its position needs to be changed.

A. PERFORMING IMAGE REGISTRATION

The process of image registration refers to the procedure of geometrically aligning the coordinate system of two or more images. Given two images, one image is selected as the reference image R and the other is selected to be the floating F. The floating image is transformed by some linear transformation until it is spatially aligned with the reference image R. Let $T\vec{\alpha}$ be a linear transformation with the vector parameter $\vec{\alpha}$. The number of elements in $\vec{\alpha}$ determines the degree of freedom. For this 2D application an affine transformation with six degrees of freedom was adequate to perform the registration. The transformation is given as:

$$F' = T_{\vec{\alpha}}(F)$$

OR

$$\begin{bmatrix} x' \\ y' \\ 1 \end{bmatrix} = \begin{bmatrix} a_{11} & a_{12} & t_x \\ a_{21} & a_{22} & t_y \\ 0 & 0 & 1 \end{bmatrix} \begin{bmatrix} x \\ y \\ 1 \end{bmatrix}$$

where (x, y) are the co-ordinates in the floating image F and (x', y') are the co-ordinates int the transformed floating image F'. It is obvious that the selection of $T\vec{\alpha}$ is not restricted to the transformation matrix. Other transformation matrices can be used based on the assumptions made regarding the nature of the mis-registration.

An appropriate criterion function which is able to determine the degree of mismatch between the reference image R and the floating image F' must be chosen. MI was chosen as an adequate function based on its previous success in the literature as being a good measure for multi-modal applications. MI is a popular measure of comparison because of its ability to measure the similarity between the two images while somewhat ignoring the mismatch of intensities across modalities. For a given reference image R, floating image F' and transformation $T\vec{\alpha}$, the MI is calculated by:

$$I(R, F', T_{\vec{\alpha}}) = \sum_{r,f'} p_{R,F'}(r, f') \log \frac{p_{R,F'}(r, f')}{p_R(r) \cdot p_{F'}(f')} \qquad \textbf{(3.5)}$$

Where the transformation that correctly registers the images is given by

$$T_{\vec{\alpha}_{reg}} = \arg\max_{T_{\vec{\alpha}}} I(R, F', T_{\vec{\alpha}}) \qquad \textbf{(3.6)}$$

After $T\vec{\alpha}_{reg}$ it is then applied to the floating image F to produce F'_{reg}. The reference image R and registered floating image F'_{reg} are compared to test how well the registration process performed.

B. CALCULATING MI USING PIXEL VALUES

The first step in the registration process was to make an initial guess for the registration transformation. This helped in avoiding local minimums and speed up the convergence of the optimization. Image moments were used for initial transformation. The initial value of the translation in x and y directions was estimated by comparing the center of gravity (COG) of the two images. The initial scale in both the x and y directions were set to 1. Given the initial guess

$$\vec{\alpha}_o = \begin{bmatrix} a_{11_o} & a_{12_o} & a_{21_o} & a_{22_o} & t_{x_o} & t_{y_o} \end{bmatrix}$$

an optimization routine was used to find the maximum value of I (or minimum value of $-I$) for the transformation $T\vec{\alpha}$ as shown in Eq. (3.6). The MI given in Eq. (3.5) is calculated by generating a normalized joint histogram based on the intensities of both the reference image R and the transformed floating image F'. Local minima in the criterion function were eliminated by blurring the joint pmf as well as blurring the images before calculating. This prevented irregular jumps in the MI function. It was also important to find a function that would make the MI smooth at the minimum. The following function was used to ensure that the global minimum of the optimization function had no irregularities.

3.8 REGISTRATION METHODS USED

In this technical report focus is on describing two image registration techniques that have been used for aligning the images. The two methods used are:

- **Skeleton Based Registration**
- **Pixel Based Registration**

In the skeleton based method initially we have time series images 2D MIP images of dendritic spines. The first step is to obtain the skeleton of these images which is a process of reducing foreground regions in a binary image to obtain a skeletal remnant that preserves the connectivity of the original image while throwing away most of the foreground pixels/voxels. The next step is to register the skeleton of these time series images using mutual information as the criterion function. Basically this technique involves affine

transformation with six transformation parameters and our motive is to obtain values for the parameters which maximizes the mutual information, i.e. optimal values for those parameters which make the registration quality better. Now, since we have obtained the optimal transformation parameters which have successfully registered the skeleton we can utilize these parameters to appropriately register the input images as well by transforming them. The advantage of using this skeleton based registration is that it takes relatively lesser amount of time to register the skeleton since it is single-pixel width.

The pixel based registration is very much similar to the skeleton based registration the biggest difference being that computing the skeleton is not needed in this approach. This approach takes a little bit more computation time as more number of pixels are needed to be processed. The quality of registration obtained is very much higher and therefore segmentation of dendritic spines becomes much easier in time series images.

3.8.1 SKELETON BASED REGISTRATION

The first approach that has been adopted to register the time series images of dendritic spines is the skeleton based registration approach. As we have discussed earlier the skeleton is a stick like figure which resembles the original shape of the object and also the skeleton being of single pixel width has relatively much lesser number of pixels than the original image. Therefore, the registration of time series images being in general a computationally expensive procedure becomes a lot faster since only the skeleton needs to be registered. The first step in the skeleton based registration approach is to obtain the skeleton. The data that has been used contains time series images of the same dendritic segment at 3 different instants T0, T1 and T2. Using the GUI that we have developed we can click on the 1st image at T0 time instant so it will generate a red seed point at that particular co-ordinate in the image so the red point also falls on the same spot of the other images at instants T1 and T2 as well. Now, since the images being unregistered the red spot on T0 will be marked at a different place when compared to T1 and the spot on T1 will be at a different point than T2. Basically there is a sort of misalignment. This can result from lens and sensor distortions or differences between capture devices. The figure 3.10 shows this concept of misalignment with the help of red seed points at T0, T1 and T2 instant.

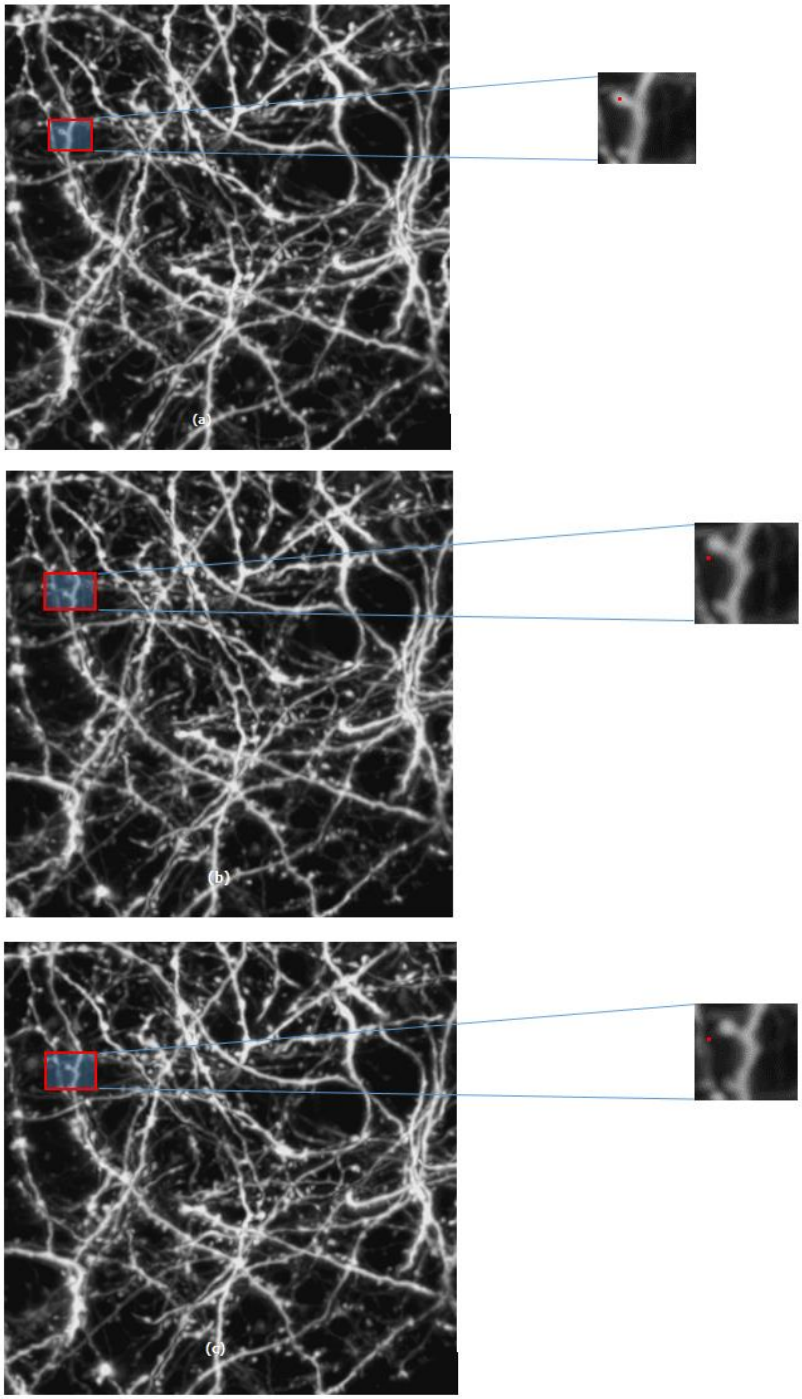

Fig 3.10 Red seed point at some spot in T0 where it appears in images at instants T1, T2 (a) seed point location in T0 (b) seed point location in T1 (c) seed point location in T2

Now using the Skeletonization algorithm as discussed in section 3.6 we obtain the skeleton of each and every image for time instant T0, T1 and T2. Then we try to registering the

$(i+1)^{th}$ with the i^{th} transformed image of the skeleton. In this process we obtain the optimal transformation parameters and these parameters are used to transform the original grayscale images as shown in figure 1.2 of *chapter 1*. The skeleton of the images are shown in figure 3.11 and the registered images are shown in figure 3.12.

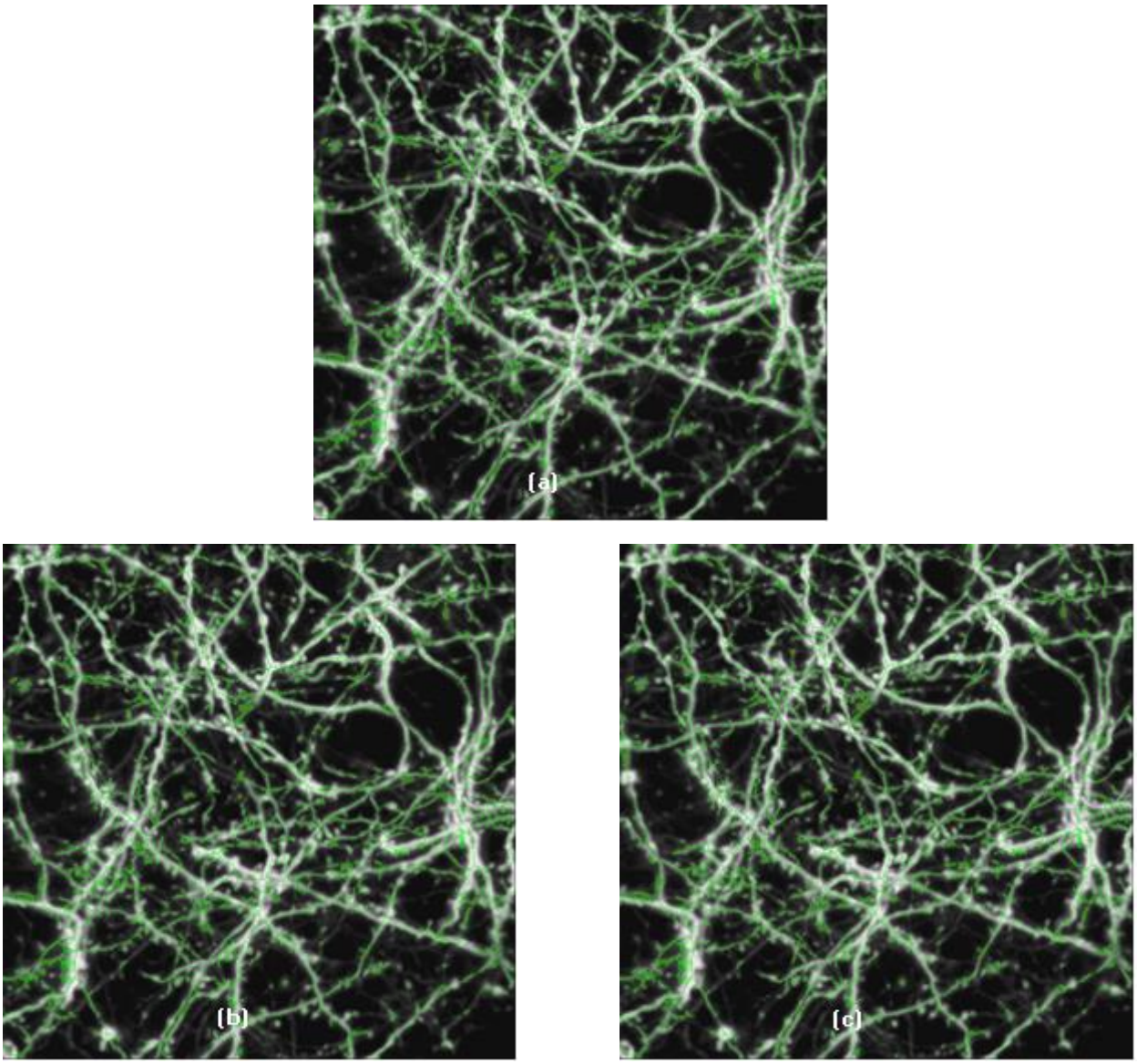

Fig 3.11 Skeleton of MIP images for time series images along with their detected junction points marked in red (a) skeleton for MIP image at T0 instant (b) skeleton for MIP image at T1 instant (c) skeleton for MIP image at T2 instant

As we can see that quality of skeletonization obtained is not very proper since the quality of binarization is an issue of medical images since the very beginning. Nevertheless this approach is very fast and the quality of registration obtained as shown in figure 3.11 is quite

good. The results will be further better in the pixel based registration approach in section 3.8.2

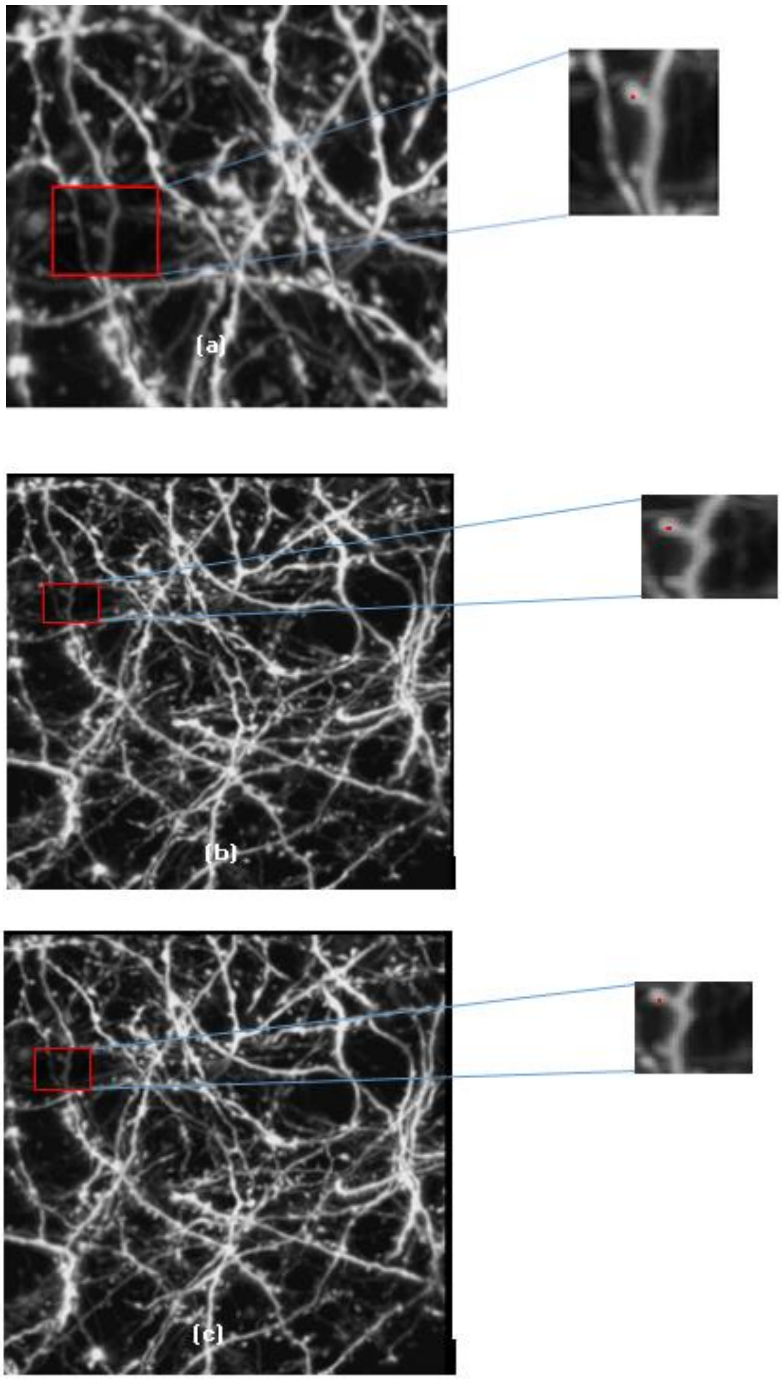

Fig 3.12 Red seed point at some spot in T0 on mouse click appearing at instants T1, T2 after alignment (Skeleton Registration) (a) seed point location in T0 (b) seed point location in T1 (c) seed point location in T2

3.8.2 PIXEL BASED REGISTRATION

Pixel Based Registration is the second approach that has been used to register the 2D time series MIP images of dendritic spines. As mentioned earlier the images of different time instants have certain amount of misalignment between them. Consider we have **N** images of different time stamps. Then there is misalignment between each **i-th** and **(i + 1)-th** image. We need to correct this misalignment which may be due to lens and sensor distortions or differences between capture devices. Here, in this approach the **i-th image** is the *fixed image* and the **(i + 1)-th** image is the *moving image.* So, we will transform the *moving image* till it bears close resemblance with the *moving image.* The idea is to find a spatial mapping i.e. elements in *moving image* into meaningful correspondence with elements in a *fixed image.* Registration is necessary in order to be able to compare or integrate the data obtained from these different measurements.

The overhead of *Skeletonization* is not there and the alignment quality is much better. So, this method skips the requirement of binarization which is ultimately used as one of the initial steps in *Skeletonization. Image Binarization* has been an issue for medical images since medical images consist of objects which are microscopic and there are varying regions of intensity in these images. Also due to the conversion of 3D stack to obtain 2D images using Maximum Intensity Projection (MIP) there is a certain amount of loss of information which is not negligible. In this method of *registration* comparison of intensity patterns via **Mutual Information** (MI) is done. This method is a bit more computationally expensive as more number of pixels are needed to be processed as compared to the skeleton based approach. Since the skeleton being of single pixel width consists of fewer number of pixels so in the actual transformation lesser amount of pixels need alignment. But in the pixel based approach relatively much larger number of pixels need processing. The quality of registration obtained is very much higher. When we later perform the segmentation of dendritic spines becomes possible because now the images have been aligned. It would be impossible to perform segmentation in images of different time stamps if the images were not properly aligned. After the alignment the segmentation quality in the images of different time stamps becomes much superior. The figure 3.13 shows the registration quality as a result of pixel based registration.

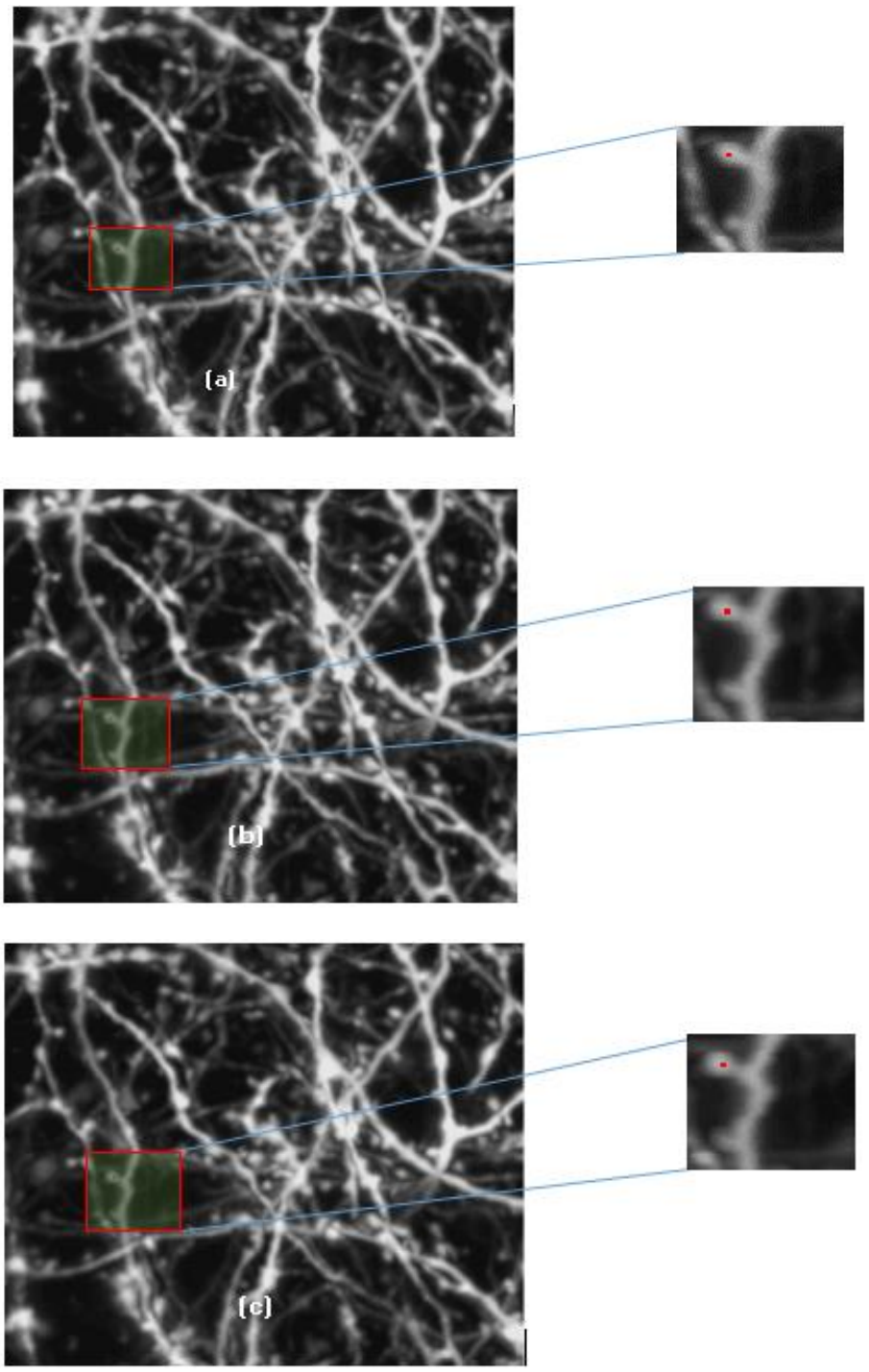

Fig 3.13 Red seed point at some spot in T0 on mouse click appearing at instants T1, T2 after alignment (Pixel Based Registration) (a) seed point location in T0 (b) seed point location in T1 (c) seed point location in T2

CHAPTER 4

METHODOLOGY

Our proposed method is designed to analyze individual dendritic spines automatically in time series images. This method first performs image registration of time series images which helps to rectify the misalignment during image acquisition since images are captured under variable conditions that might the camera perspective or the scene's contents. Therefore, after registration spine tracking becomes easier in the time series images since the images have been aligned spatially. The next objective is to segment the dendritic fragment which has been done using the theoretical foundation of digital topology like Fuzzy Distance Transform (FDT), Center of Maximum Balls (CMB), etc. Spine segmentation has been done by developing an adaptive version of the flood-fill algorithm. Lastly the skeleton of these time series images has been utilized to calculate individual spine features like spine area, head width, neck length, etc. which can help us to closely monitor morphological changes occurring in dendritic spines (i.e. spine plasticity). Spine classification and numbering is also done utilizing the skeleton and the individual spine features.

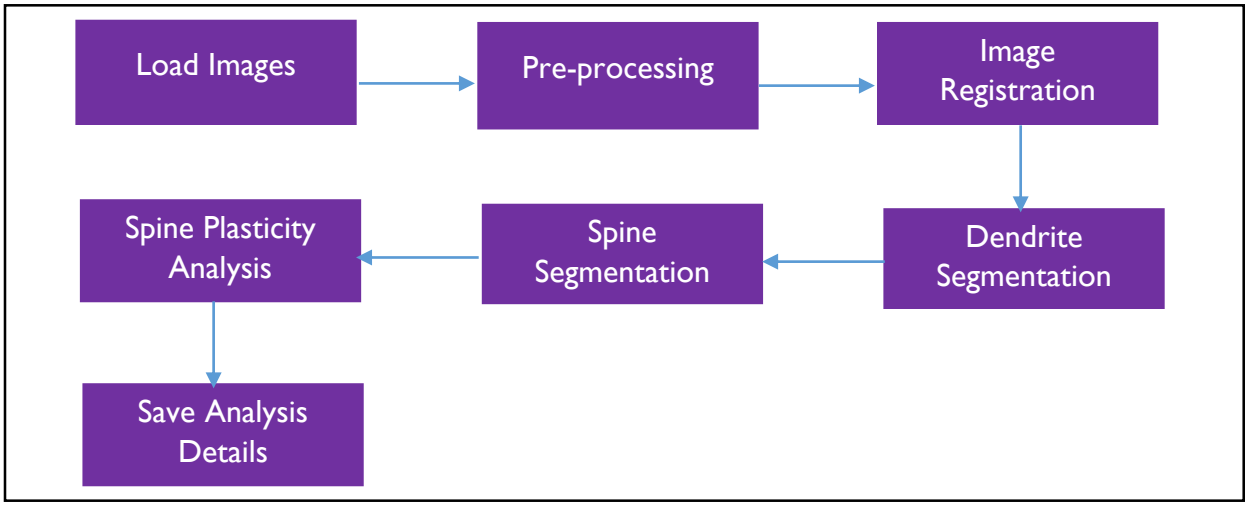

Fig 4.1 Flow chart for quantitative analysis of spine plasticity in 2D images of dendritic spines at different time stamps

4.1 PRE-PROCESSING

The purpose of this is to obtain a noise free 2D MIP image of dendritic spines. 3D microscopy followed by is commonly used to study different biological objects such as cells, neuron and tissue.

A 3D stack contains all pieces of information needed to reconstruct a focused 2D image. To create a 2D image from 3D stack a projection in the z direction is often preferred as it contains the highest amount of information. Above 80 percent of the biologist community use MIP, to reduce a 3D stack into a single 2D image. MIP retrieves the level of maximum intensity along the z axis for each x, y position. The image of 3D stack is called the index map while the image made of intensity values corresponding to that index map is called the projection.

MIP is widely adopted as it is the simplest method of z-projection, parameter free, fast and straightforward to use as it is implemented in NIH Fiji/ImageJ7 and in many other softwares. Our dataset is generated by imaging different neuron from rat dissociated hippocampal cultures using a confocal light microscope, before and after chemically induced long-term potentiation (cLTP).

Images have been captured at three different time instants, initially at time instants T0, T1 and T2 to identify the structural and morphological changes in the chemical solution over time. Spines have various shapes, and spine images are often not of very good quality, hence it is very challenging to detect spines in these images. During image processing MIP of the confocal z-stack used to convert the 3D stack image into a 2D image and Gaussian de-noising has been performed on the 2D MIP image. The figure 4.2 shows the time series images of dendritic spine at three different instants T0, T1 and T2.

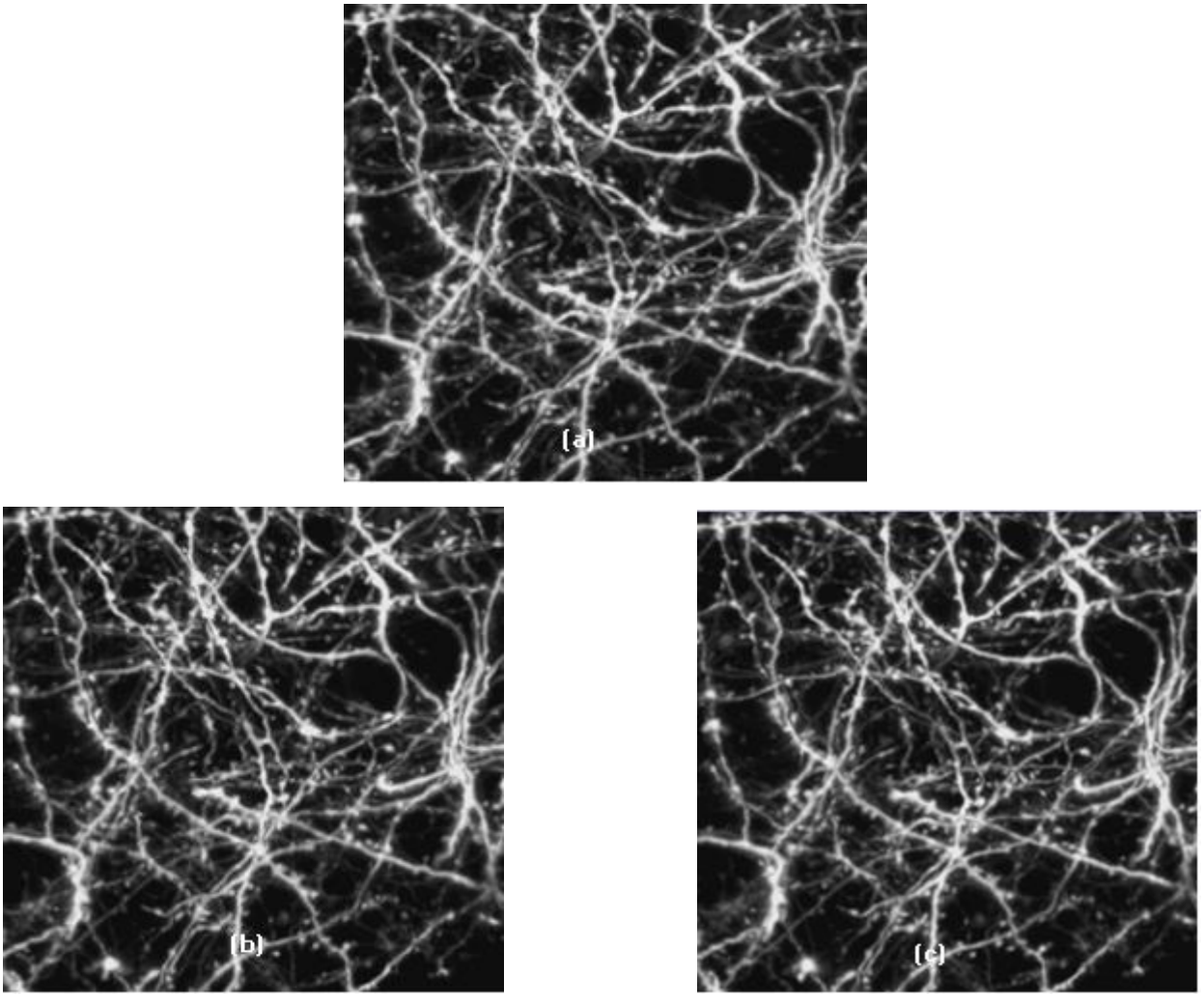

Fig 4.2 2D MIP images of dendritic spines at different time instants (a) MIP of cell at T0 (b) MIP of cell at T1 (c) MIP of cell at T2

4.2 IMAGE REGISTRATION

As it has been already discussed in the *chapter* 3 that image registration has been used because it can spatially align time series images of different time instants**.** The main motive of our work is to track spine behavior in time series images which would be impossible if the spatial location of the spines is not properly aligned which is what we see in case of the data that we have before applying our image registration algorithm. Image registration helps in rectifying this alignment. The figure 4.3 this concept of misalignment with the help

of red seed points at T0, T1 and T2 instant and the figure 4.4 shows that the images have been aligned properly after the image registration algorithm has been applied to the images at time instant T0, T1 and T2.

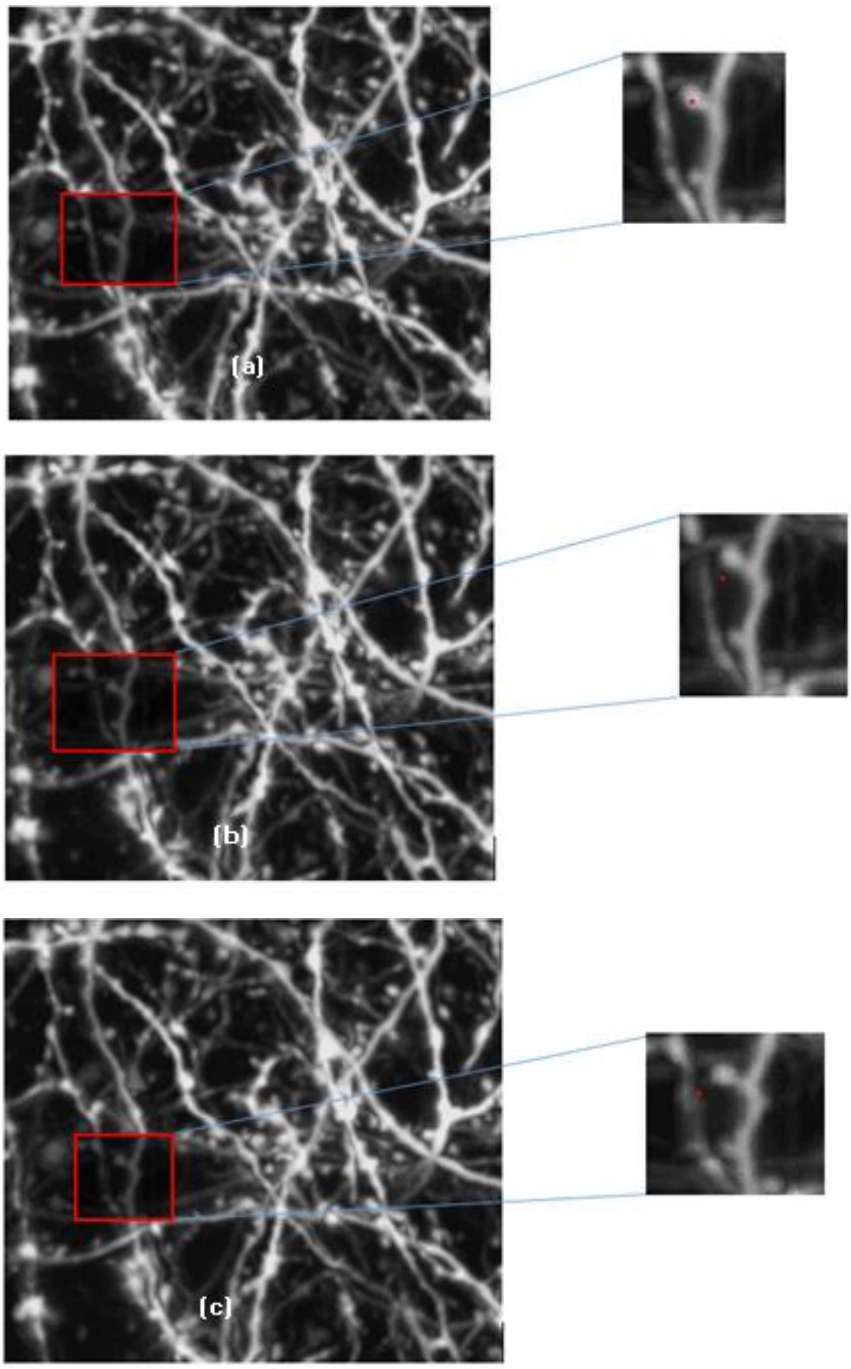

Fig 4.3 Red seed point at some spot in T0 on mouse click appearing at instants T1, T2 before alignment (Registration) (a) seed point location in T0 (b) seed point location in T1 (c) seed point location in T2

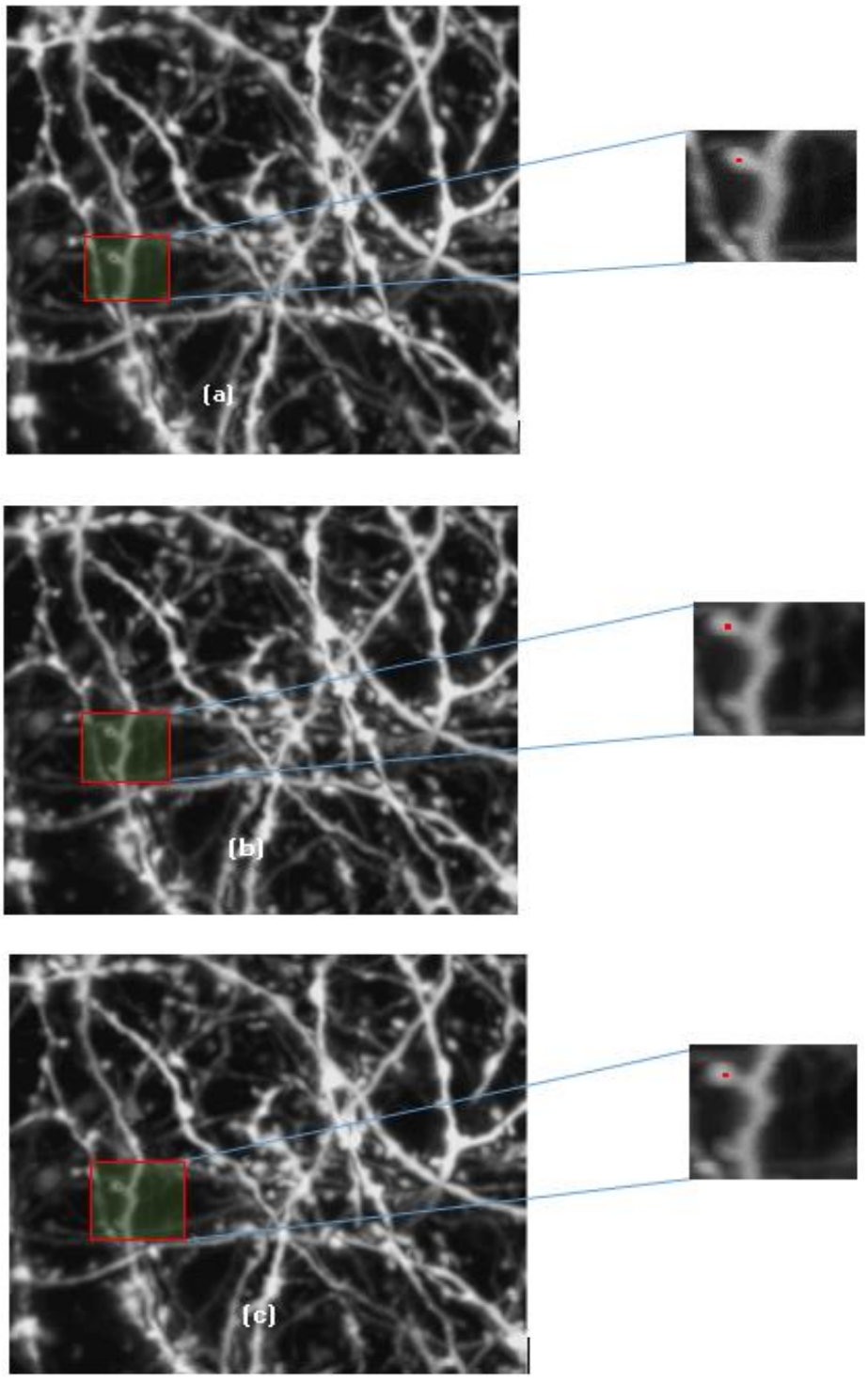

Fig 4.4 Red seed point at some spot in T0 on mouse click appearing at instants T1, T2 after alignment (Registration) (a) seed point location in T0 (b) seed point location in T1 (c) seed point location in T2

4.3 ENHANCING REGION OF INTEREST LOCALLY

Generally medical images are of not great quality. The images are mostly of such poor quality that our concerned objects are not clearly visible. In our case the images that we have acquired are no exception. Since one of our major motives include dendrite and spine segmentation at least the quality of the concerned region of interest (ROI) had to be enhanced which has greatly helped in the dendrite and spine segmentation. In the GUI a user can click anywhere on the image to select a region with similar colors. We also have a tolerance track bar in the GUI which provides for the range of allowable deviation from a color so as to facilitate the selection of a region of our interest.

After the images have been registered in the GUI a user can click at any point in the image which is the seed point. Now, taking that seed point we run our flood-fill algorithm with a certain tolerance limit which gives the control to the user as to how much deviation in intensity value from the seed point's intensity value has to be allowed. Therefore, a region with similar colors (as per tolerance) is selected and our flood-fill will replace those old pixel values with the new pixel values that we have supplied in the flood-fill function as parameter. This change happens in each and every image since we have time series images and the advantage is that we just need to place a single click on the very first image at T0 instant as shown if figure 4.2(a) and the enhancement is reflected in the images at time instants T1 and T2 as shown in figure 4.2(b) and 4.2(c). Also, in the flood-fill function we supply as parameters an operation mask that should be a single-channel 8-bit image, 2 pixels wider and 2 pixels taller than image. This mask is nothing but a binary image which indicates which pixels have been re-colored by the flood-fill algorithm. Flood-filling cannot go across non-zero pixels in the input mask. For example, an edge detector output can be used as a mask to stop filling at edges. On output, pixels in the mask corresponding to re-colored pixels in the image are set to white (intensity value = 255). It is therefore possible to use the same mask in multiple calls to the function to make sure the filled areas do not overlap. The enhanced region of interest of images as shown in figure 4.2 along with their masks is shown in figure 4.5.

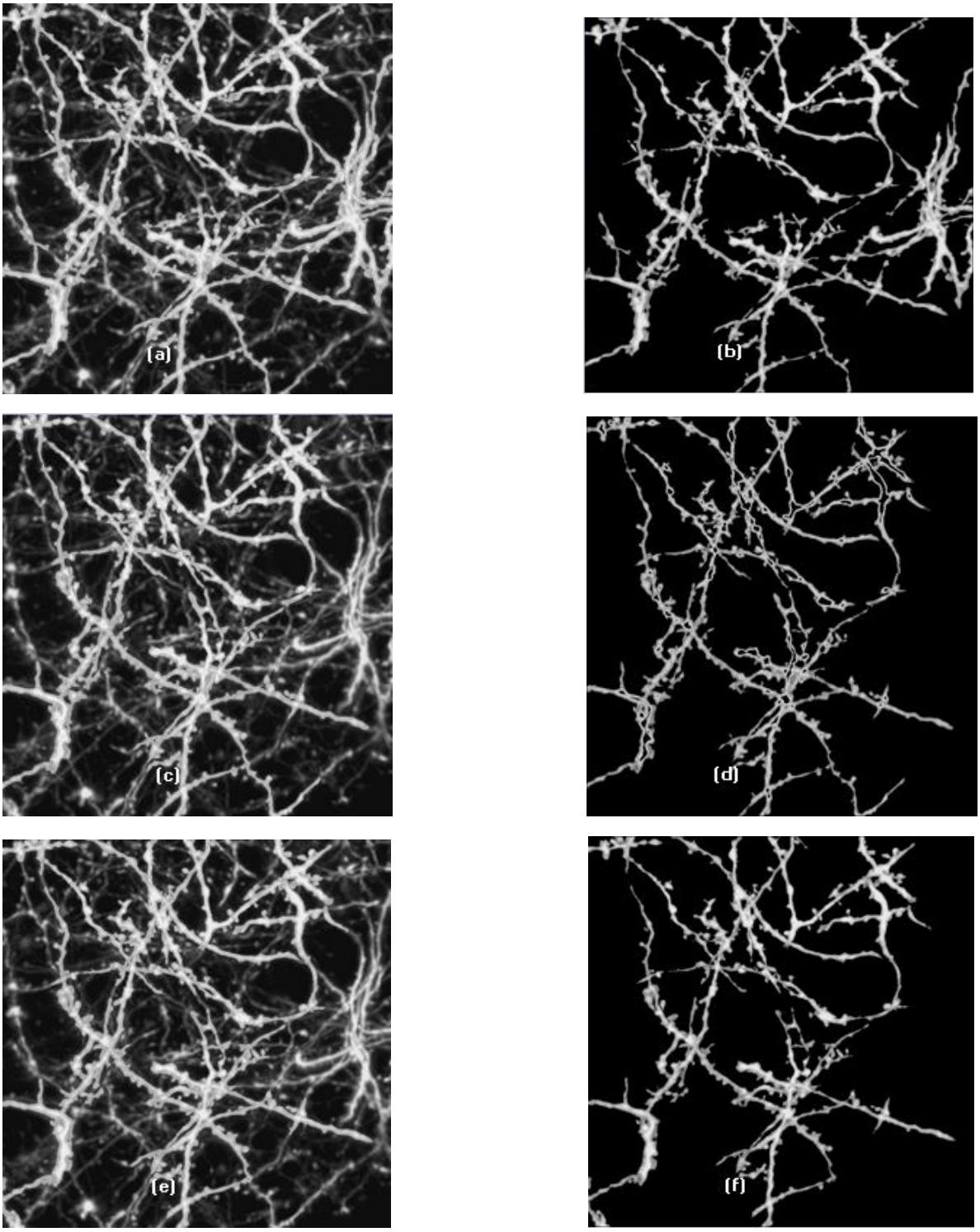

Fig 4.5 Enhanced region of interest and its mask with tolerance level 76 for dendritic spine images at instant T0, T1 and T2 (a) enhanced image at T0 (b) mask for T0 (c) enhanced image at T1 (d) mask for T1 (e) enhanced image at T2 (f) mask for T2

The mask that contains the information about the points that are re-colored is now utilized to detect the boundary points or the contours. Contours can be explained simply as a curve joining all the continuous points (along the boundary), having same color or. These contours help us to understand the morphology of dendritic spines in a more detailed way and is an elegant approach since it will make the task of dendrite and spine segmentation much easier later. The figure 4.6 shows the enhanced region of interest of images along with their detected contours.

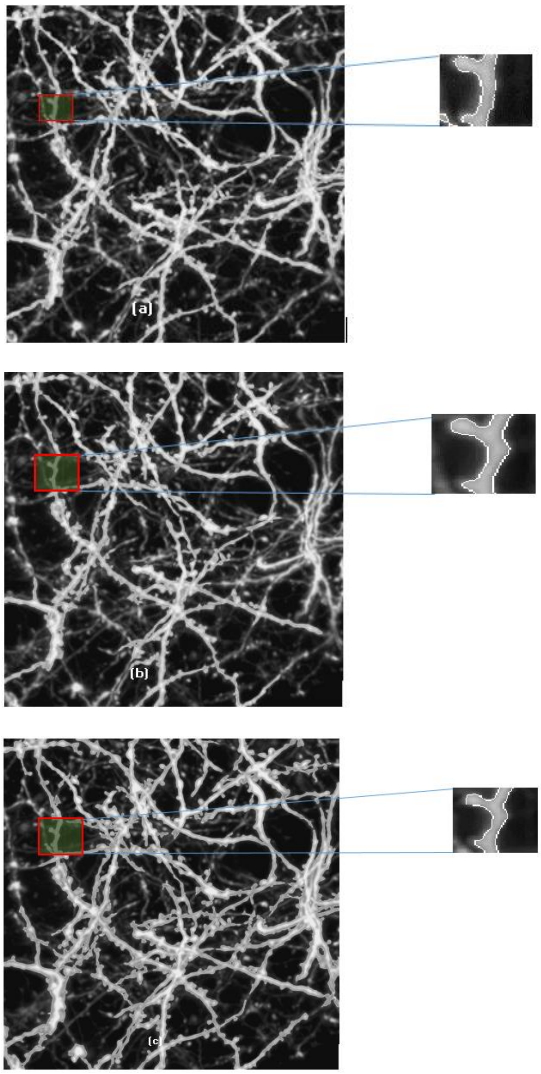

Fig 4.6 Enhanced region of interest and their contours with tolerance level 76 for dendritic spine images at instant T0, T1 and T2 (a) enhanced image at T0 and detected contour (b) enhanced image at T1 and detected contour (c) enhanced image at and detected contour

4.4 DENDRITE SEGMENTATION

After enhancing the ROI locally the next task is to segment the dendrite. In our work we have done color-based segmentation approach. For this we have utilized certain concepts like Fuzzy-Distance Transform, Center of Maximum Balls, etc. to segment the region between the source and the destination points using a shortest path algorithm which is very much like Breadth-first search with some minor modifications. The figure 4.6 shows the segmented dendrite of the time-series images.

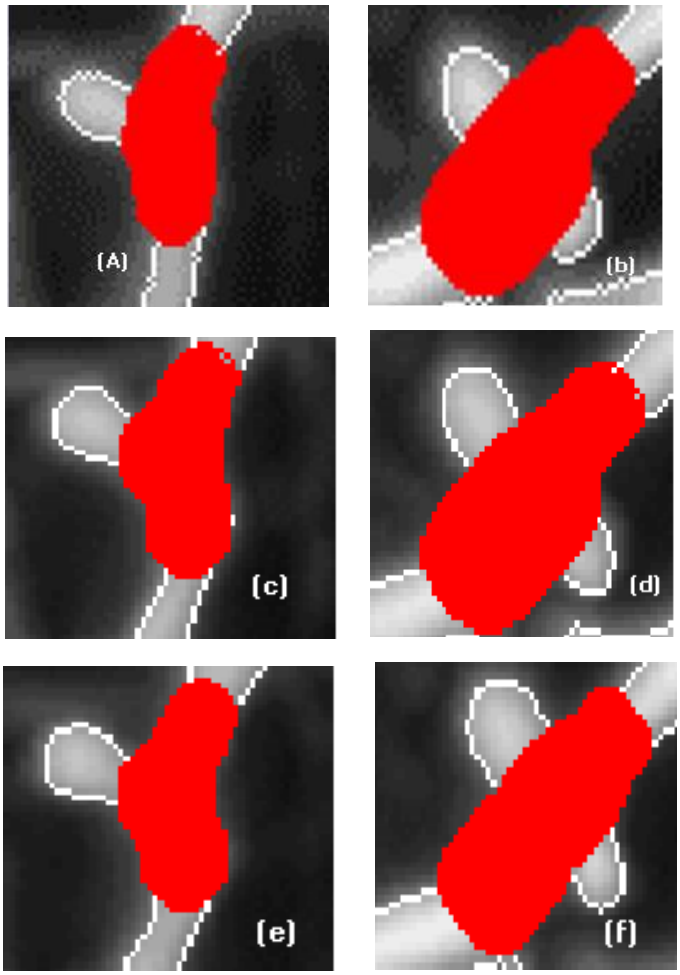

Fig 4.7 Segmented dendrite of 3 different time-series images at instants T0, T1, T2 (a), (b) dendrite segments at T0 instant (c), (d) dendrite segments at T1 instant (e), (f) dendrite segments at T2 instant

What we have essentially done in this approach is with the help of GUI selected 2 points one source and destination. Then, we have calculated the shortest path between those 2 points. We have earlier calculated the FDT of the entire image so the points which are selected for the shortest path must be having some FDT value. So, we have taken these values as radius and drawn red colored filled circles so that the above results in figure 4.6 has been obtained. Let's discuss the shortest path algorithm we have utilized.

ALGORITHM FOR SHORTEST PATH

Input: A 2D grayscale image I having an object region O with 2 marked points p & q in O.

Output: Segmented dendrite in concerned ROI between p & q.

PHASE-I

$S(x, y)$: Starting point.

$E(x, y)$: End point.

$\mathcal{O}$: Set of object pixels.

Q: A queue

D: An image where each pixel value represents its distance from the starting point.

NN: An image where each pixel stores position of its neighbour nearest to the starting point.

$$Cost(p, q) = \frac{\mu(p, q)}{FDT(q)}$$

$\mu(p, q)$: Distance of the link between p, q

$FDT(q)$= Distance transform value of q from the background.

1. $\forall p \in \mathcal{O}$
   I. $D(p) = \infty$
   II. $NN(p) = NULL$
2. For $p = S$
   III. $D(p) = 0$
   IV. $NN(p) = p$
   V. PUSH p in Q
3. while Q is non-empty
   I. POP p from Q

II. $\forall q \in N^*(p) \cap O$
   a. If $D(q) > D(p) + cost(p,q)$
      i. $D(q) = D(p) + cost(p,q)$S
      ii. $NN(q) = NN(p)$
      iii. PUSH q in Q

PHASE-II

For end point, $p = E$,

I. Initiate a path π=p and set $q = p$;
II. While($q! = S$)
III. {
IV. $q = NN(q)$
V. Append q in π
VI. }

Basically we have 2 points one source and one destination. We have formulated a cost function which is directly proportional to the distance of the link between two points and inversely proportional to the FDT value of the point which is our immediate goal. In this way we explore all neighbors for a particular point and try to find out the neighbor which has the least cost to be reachable. That is what is happening in 1st phase. In the 2nd phase utilizing the nearest neighbor matrix (NN) we trace back to the starting point drawing filled red circles all along the way. Therefore, the red region in the figure 4.6 shows that segmentation of the dendritic backbone is successful.

4.4 SPINE SEGMENTATION

After segmentation of the dendritic backbone next step is to segment the spines in time-series images. For that the user only needs to click on the desired spine and color-based segmentation of the concerned spine will be achieved. For this we have developed an adaptive version of the general flood-fill algorithm. When a user clicks on a spine at some point which is taken as the seed point and a 3×3 neighborhood is taken into consideration around that point and the mean and standard deviation is computed. Furthermore, a parameter sensitivity (allowable deviation) multiplied with standard deviation is subtracted from the mean becomes the *lower limit* and the sensitivity multiplied with standard deviation added to the mean gives the *higher limit*. Then, all the neighbors are evaluated if

they lie within this range and only for those neighbors which lie within this range further recursive calls to the flood-fill algorithm takes place. The algorithm is as follows:

PSEUDO CODE FOR ADAPTIVE FLOOD FILL ALGORITHM

Flood-fill (point, target-color, replacement-color, sensitivity (s)):

1. If target-color is equal to replacement-color, return.
2. If the color of point is not equal to target-color, return.
3. Set the color of point to replacement-color.
4. Calculate the *mean* and *standard deviation* of 3 × 3 neighborhood around that point.
5. Set *lower limit* = *mean* – (*standard deviation* (s.d) × *sensitivity*)

   upper limit = *mean* + (*standard deviation* (s.d) × *sensitivity*)
6. **If** the color of one step to the south of point is between lower limit and upper limit then,

   Perform Flood-fill (one step to the south of point, target-color, replacement-color, s).

   If the color of one step to the north of point is between lower limit and upper limit then,

   Perform Flood-fill (one step to the north of point, target-color, replacement-color, s).

   If the color of one step to the west of point is between lower limit and upper limit then,

   Perform Flood-fill (one step to the west of point, target-color, replacement-color, s).

   If the color of one step to the east of point is between lower limit and upper limit then,

   Perform Flood-fill (one step to the east of point, target-color, replacement-color, s).
7. Return.

The figure 4.6 shows the segmented images of dendritic spines at 3 different time instants. The **blue** colored region indicates the segmented spines. The figure 4.6(a), (c) and (e) corresponds to a single spine at time stamps T0, T1 and T2 respectively. Similarly, the figure 4.6(b), (d), (f) corresponds to another segmented spine at time stamps T0, T1 and T2 respectively. It is quite clear that the spine shape changes in the images of different time stamps. Instead we can say that **"plastic"** nature of spines is very much clear from figure 4.6.

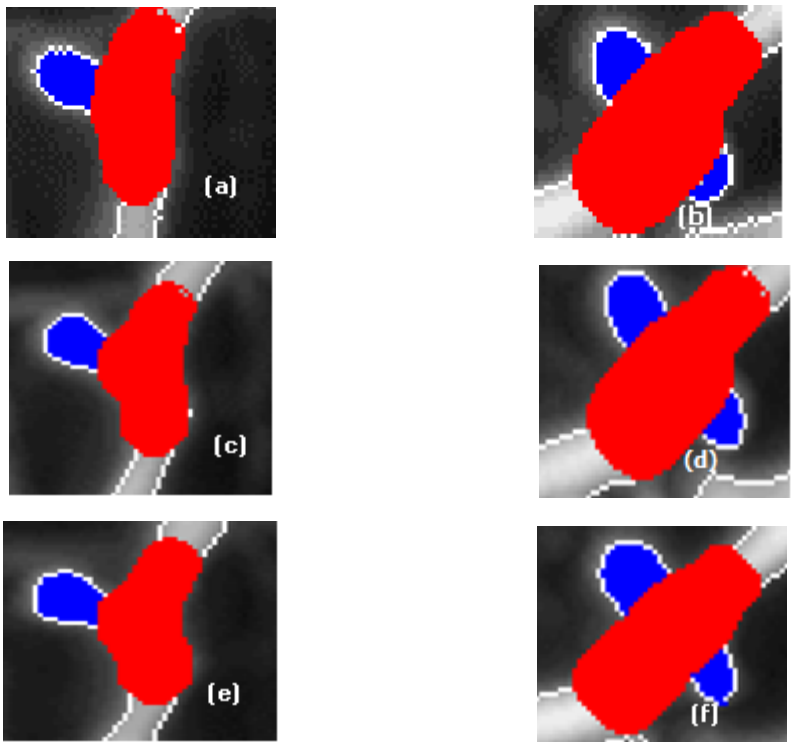

Fig 4.8 Segmented images of dendritic spines at 3 different time instants T0, T1, T2 (a), (b) spine segments at T0 instant (c), (d) spine segments at T1 instant (e), (f) spine segments at T2 instant

4.5 QUANTITATIVE FEATURE EXTRACTION

After the segmentation of the dendrites and spines has been done the next step is to extract the features from those spines. To do this we need to obtain the skeleton and also do the spine numbering. Then we can calculates individual spine features like spine length, spine area, etc. which are relevant to "plasticity analysis". The figure 4.7 shows one segmented and numbered spine in our 2DSpAn-v2 application GUI with all the features extracted.

Since we need to calculate features like spine length (S_L) and spine area (S_A) defining them is of utmost importance.

Here, S_A is nothing but the count of the pixels that are re-colored during the spine segmentation using the adaptive flood-fill algorithm as mentioned in section 4.4.

$S_L = L_L + (DT[\textit{Spine End Position}] - DT[\textit{Dendrite Junction Position}])$, where L_L is length of spine slice as obtained from the skeleton. This individual *spine slice* lengths are calculated

iteratively from each spine-dendrite junction point to the spine end are obtained from the skeleton.

Here, DT denotes the computed distance transform matrix in which each pixel has a value corresponding to nearest background pixel. DT[*Spine End Position*] denotes the distance transform value at the *Spine End Position* which is also obtained from the skeleton. DT[*Spine Dendrite Junction Position*] denotes the distance transform value at the *Spine Dendrite Junction Position* which is computed from the skeleton. The features like *spine area* and *spine length* are useful in plasticity analysis. We can observe the morphological changes occurring in the dendritic spines in images of different time stamps. The figure 4.7 shows marked spines along with the features extracted in images of time stamps T0, T1 and T2.

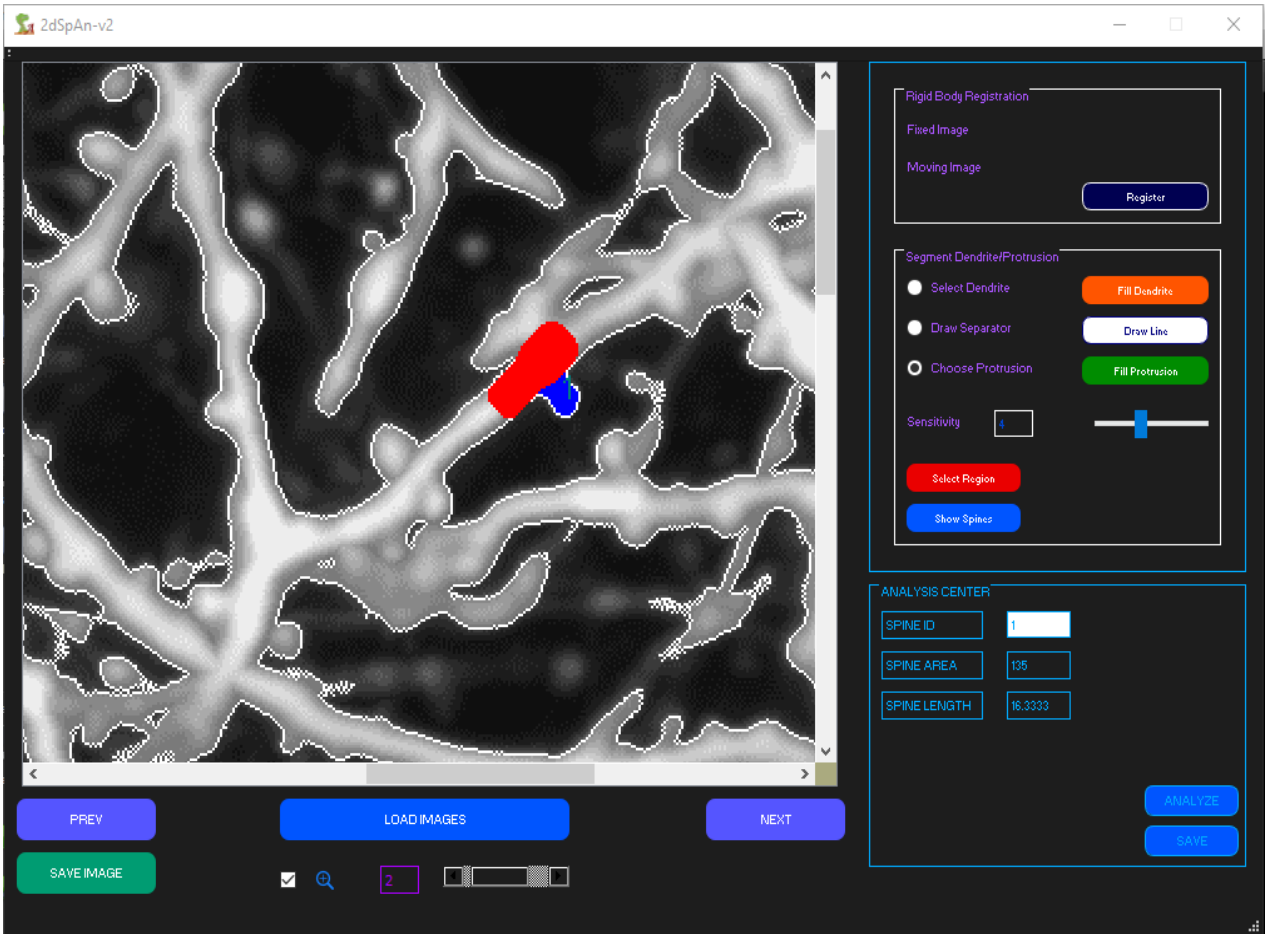

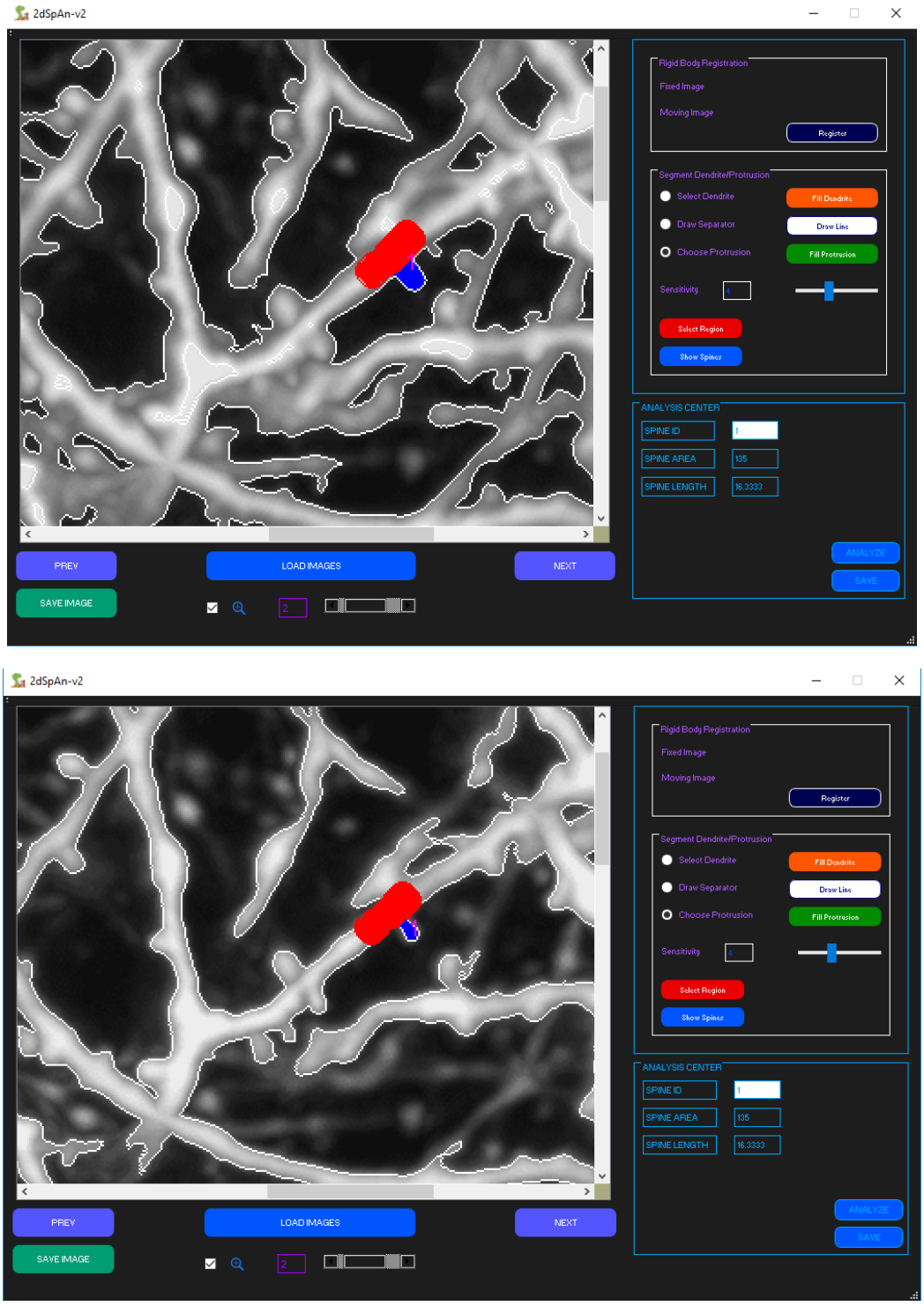

Fig 4.9 Marked spine in 2DSpAn-v2 GUI and quantitative feature extraction of marked spine at time instants T0, T1 and T2.

CHAPTER 5

GUI DESIGN AND EXPERIMENTAL RESULTS

5.1 INTRODUCTION TO QT GUI

Qt is a cross-platform framework that is usually used as a graphical toolkit and can run on any operating systems including mobile operating systems. The Qt GUI module provides classes for system integration, event handling, OpenGL and OpenGL ES integration, 2D graphics, basic imaging, fonts and text. These classes are used internally by Qt's user interface technologies and can also be used directly, for instance to write applications using low-level OpenGL ES graphics APIs. Qt is very easy to use and user don't need any high-level training to get used to with Qt. Although Qt is one of the IDE for C++ but one can integrate OpenCV, python with Qt if required.

5.2 USER MANUAL

In this section we introduce the GUI of our proposed method 2DSpAn-v2. Figure 5.1 shows the GUI followed by the description of each item on the GUI.

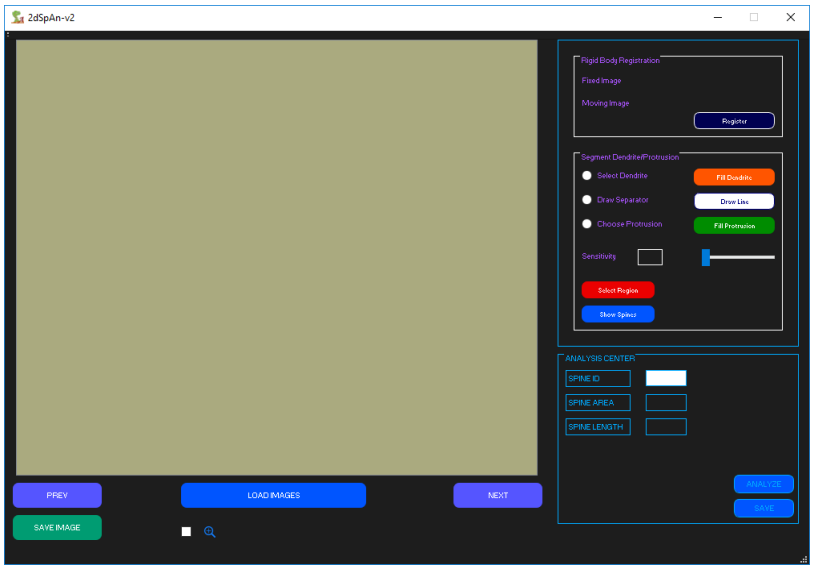

Fig 5.1 GUI of 2DSpAn-v2

Button **LOAD IMAGES**: First user needs to load the directory which contains the time series images by clicking on this button. After clicking on this button user can choose the directory and all the files from the directory will be loaded into the application. It is mandatory to keep some naming convention that necessarily indicates the time instant of

the image like T0, T1, T2, T3, etc. Since, we are working on image registration in the beginning the order of the time instants of images will be helpful for sorting them alphabetically. Suppose we have images of 3 different time instants MAX_-0001.png (1st image), MAX_-0002.png (2nd image) and MAX_-0003.png (3rd image). So, after loading the file names into our application we run our algorithm to sort the file names alphabetically so it gives the correct order so as to which image should be registered with its corresponding reference.

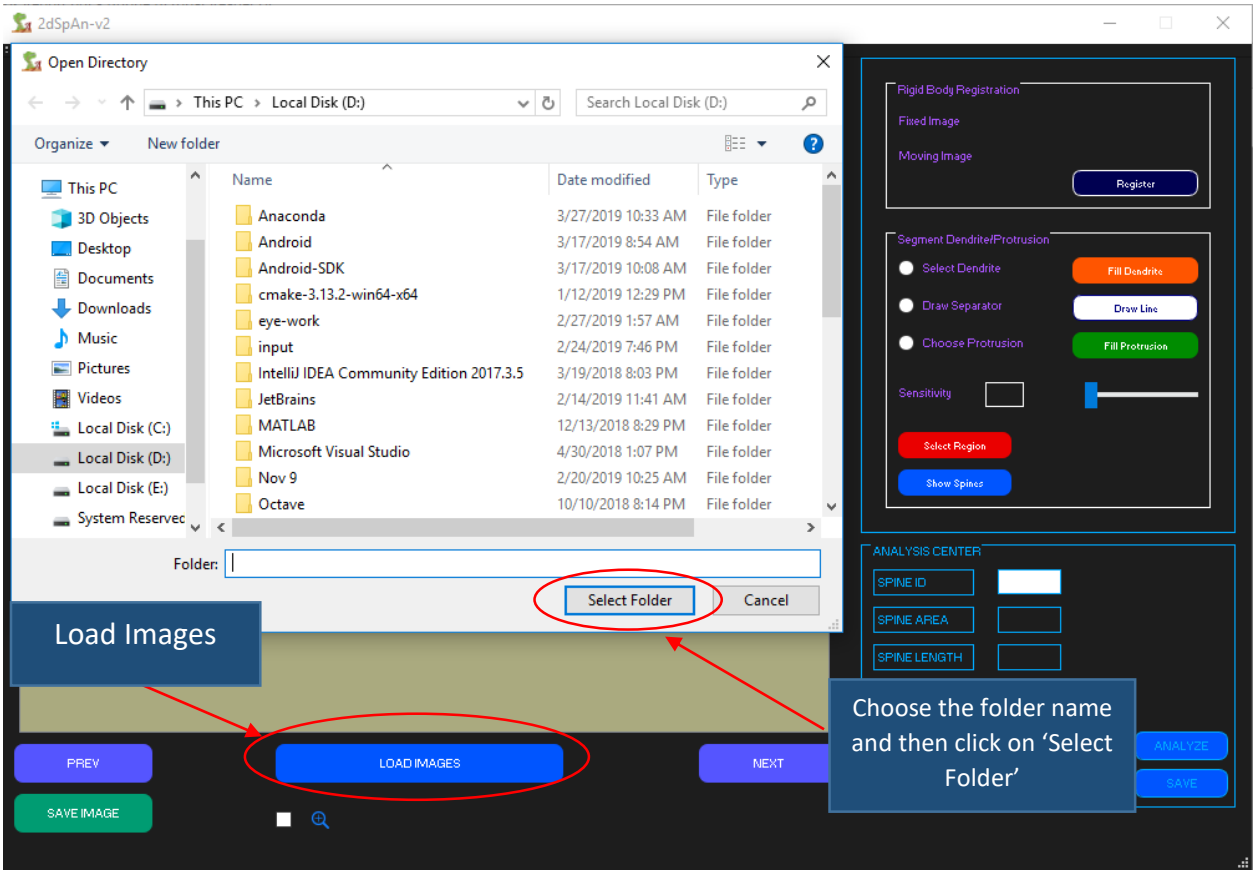

Fig 5.2 on clicking the LOAD IMAGES button

Button **PREV & NEXT:** These buttons lets the user fetch the next and previous images from the loaded list of images. We can also have a better magnified view of the images by checking the checkbox beside the magnifying glass icon. When user checked the checkbox zoom the zoom-in or zoom-out function is activated. Figure 5.3 shows how the PREV & NEXT button and also how the zoom check box works.

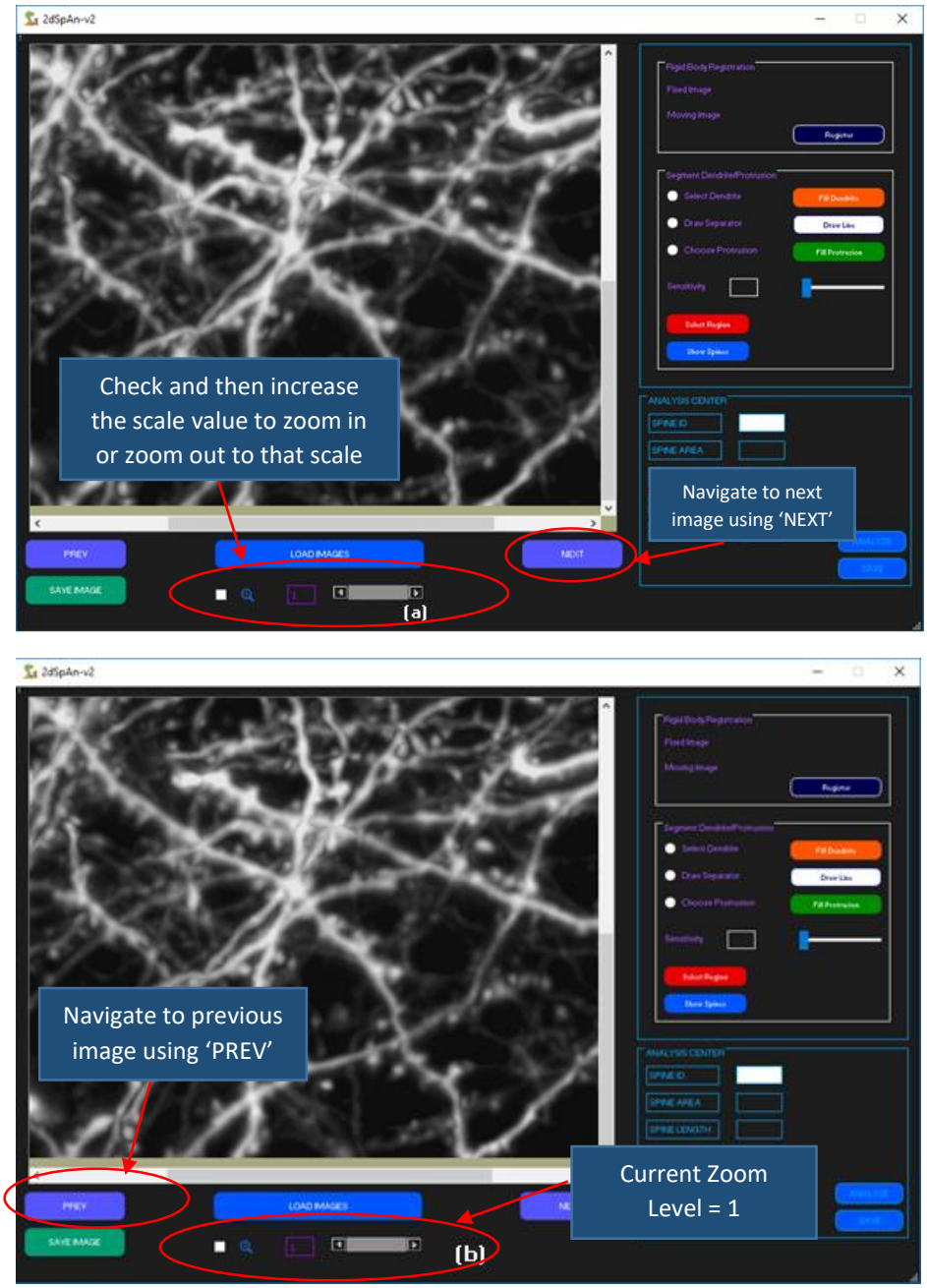

Fig 5.3 Working of PREV and NEXT buttons and zoom feature (a) Zoom Feature and NEXT button (b) Zoom Level = 1 and PREV button

Button **Register:** This button actually performs the image registration that we have discussed in the earlier chapters. It performs the alignment of two or more images of the same scene. Suppose we have images of 3 different time instants MAX_-0001.png (1st image), MAX_-0002.png (2nd image) and MAX_-0003.png (3rd image) so there will be 2 registration operations in the background the first being to align the 2nd image with the 1st

one and the second one to align the 3rd image with the 2nd one. The figure 5.4 shows the **Register** button and the figure 5.5 shows the original misalignment and figure 5.6 shows how well the image registration algorithm has performed.

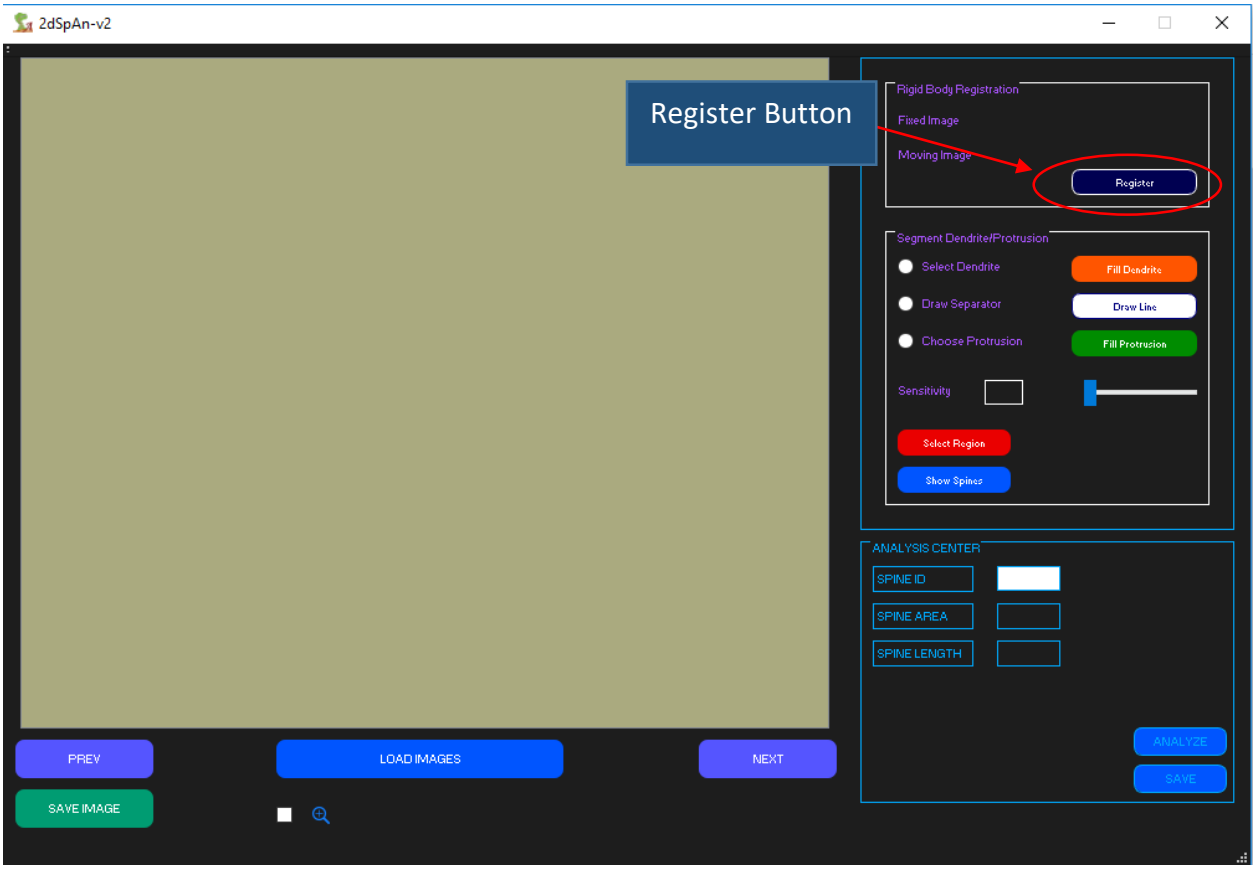

Fig 5.4 'Register' Button which performs the actual Image Registration which rectifies the misalignment between Reference & Moving Images

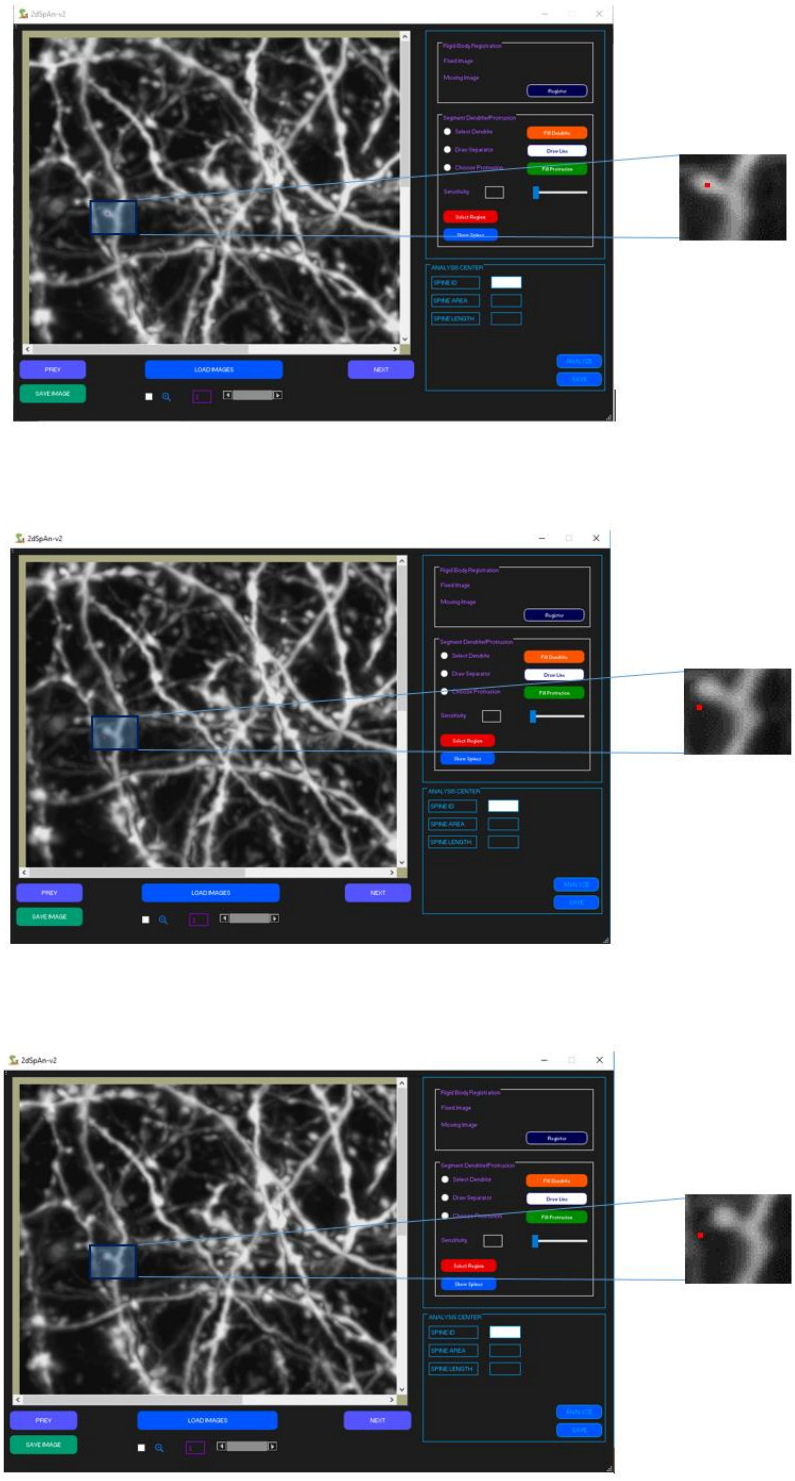

Fig 5.5 Before the register button has been clicked seed point location in the 3 time series images (a) Location at T0 (b) Location at T1 (c) Location at T2

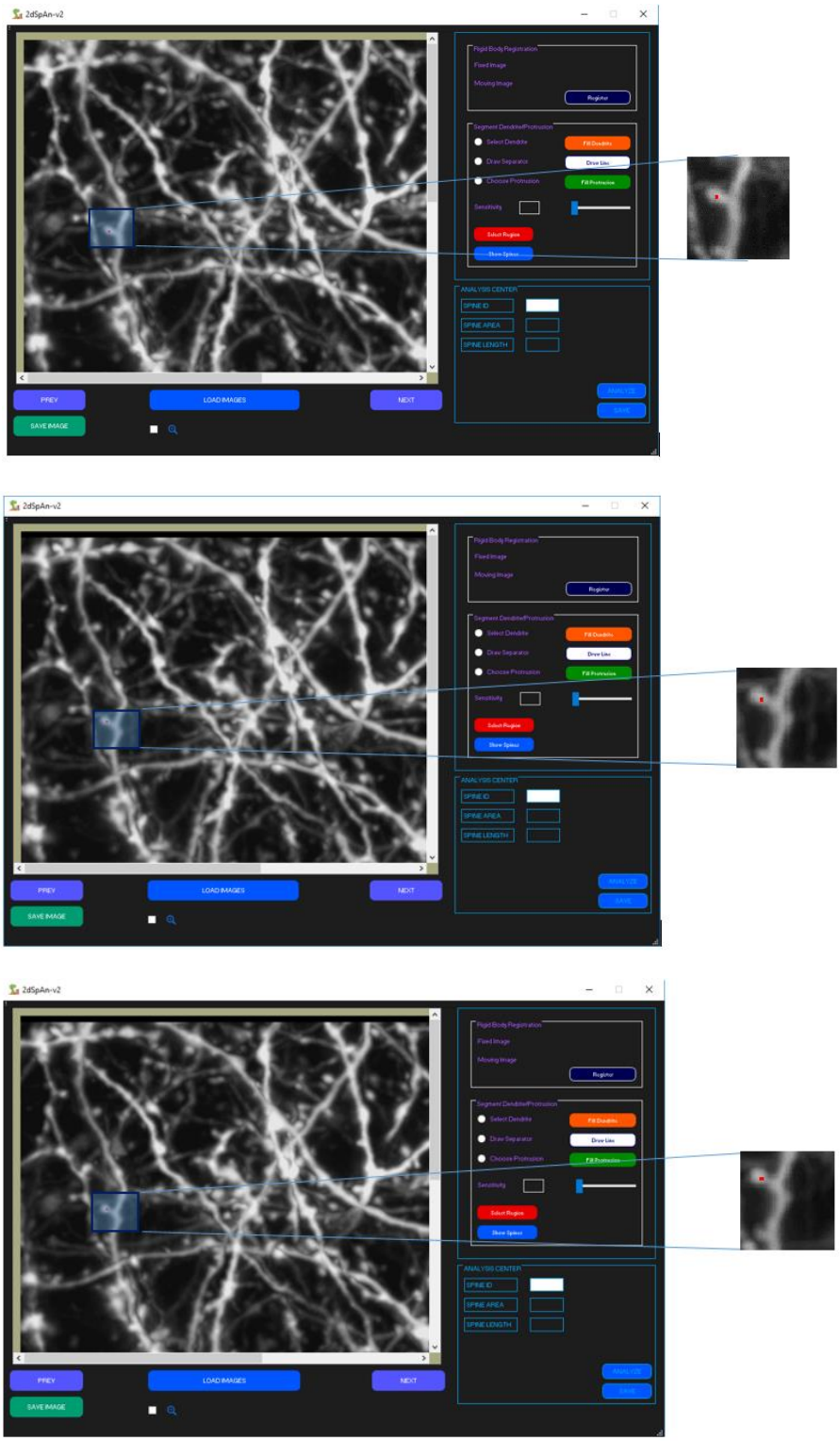

Fig 5.6 After the register button has been clicked seed point location in the 3 time series images (a) Location at T0 (b) Location at T1 (c) Location at T2

Button **Fill Dendrite:** To segment the dendrite first you need to click on the radio button **Select Dendrite** and then mark one source point and one destination point on the 1st image. These points are automatically marked on the other time series images (which are already registered) and then if the user clicks on the **Fill Dendrite** button we will have the dendrite segmentation successful. The procedure of choosing points for source and destination is shown in figure 5.7 and the segmented dendrite of T0, T1, T2 is shown in figure 5.8.

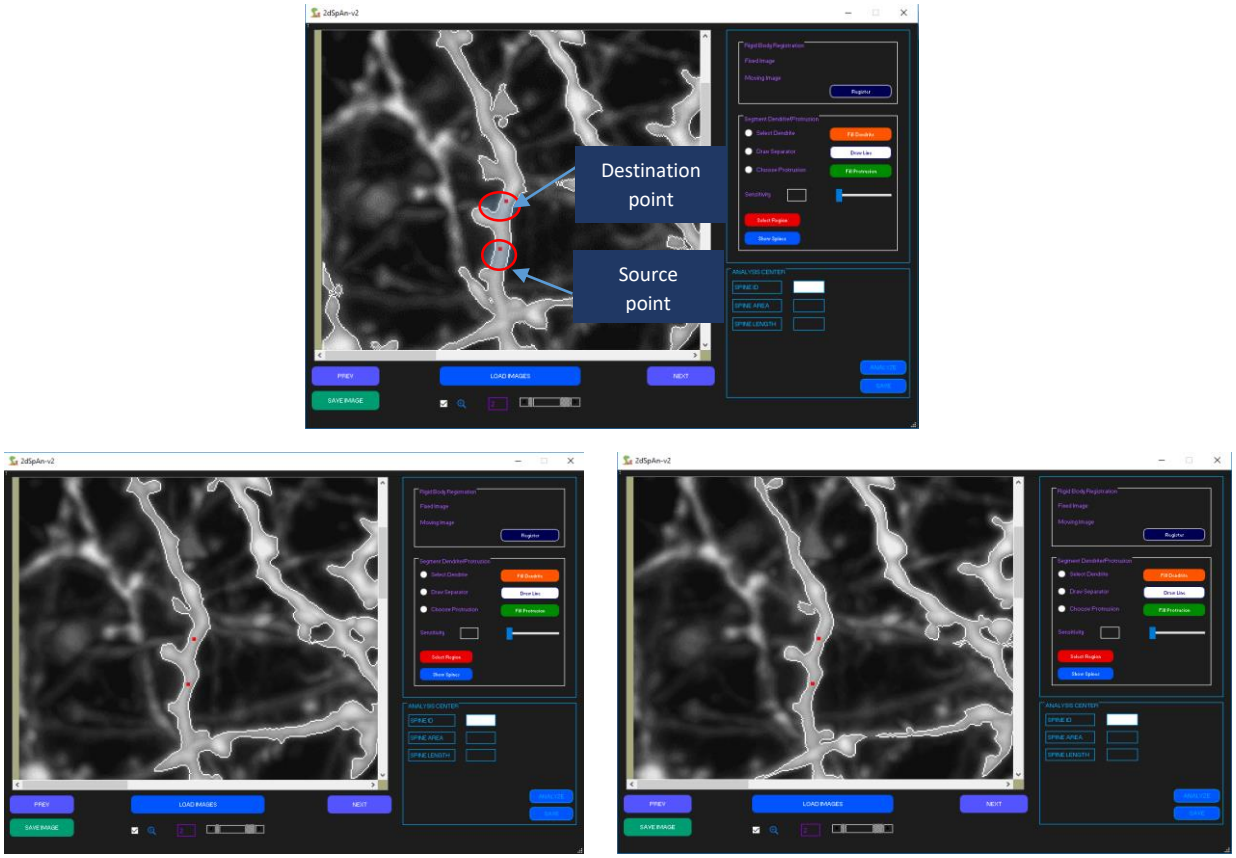

Fig 5.7 After the Select Dendrite radio button has been selected and on the T0 image source and destination points have been marked (a) Location of points in T0 (b) Location of points in T1 (c) Location of points in T2

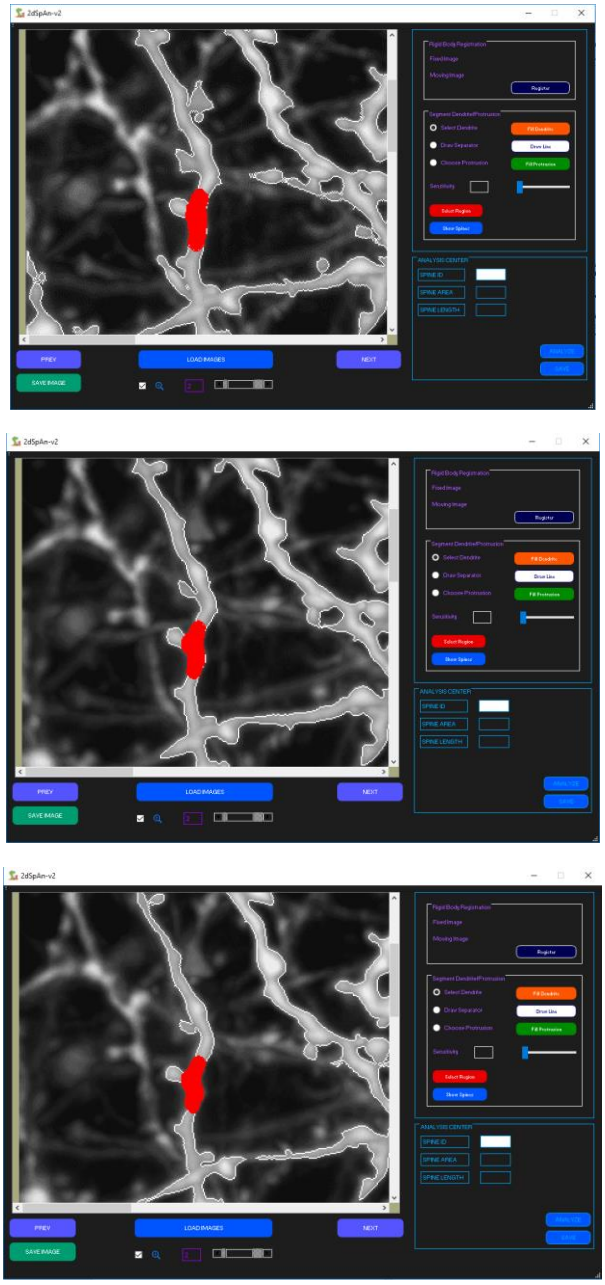

Fig 5.8 After the Fill Dendrite button has been clicked and dendrite segmentation has been done (a) Segmented dendrite in T0 (b) Segmented dendrite in T1 (c) Segmented dendrite in T2

Button **Fill Protrusion:** To segment the spine we just need to click on the radio button **Choose Protrusion** and then mark one the spine on the 1st image. These points are automatically marked on the other time series images (which are already registered) and then if the user clicks on the **Fill**

Protrusion button we will have the segmented spine. The procedure of clicking on the spine is shown in figure 5.9 and the segmented spine of T0, T1, T2 is shown in figure 5.10.

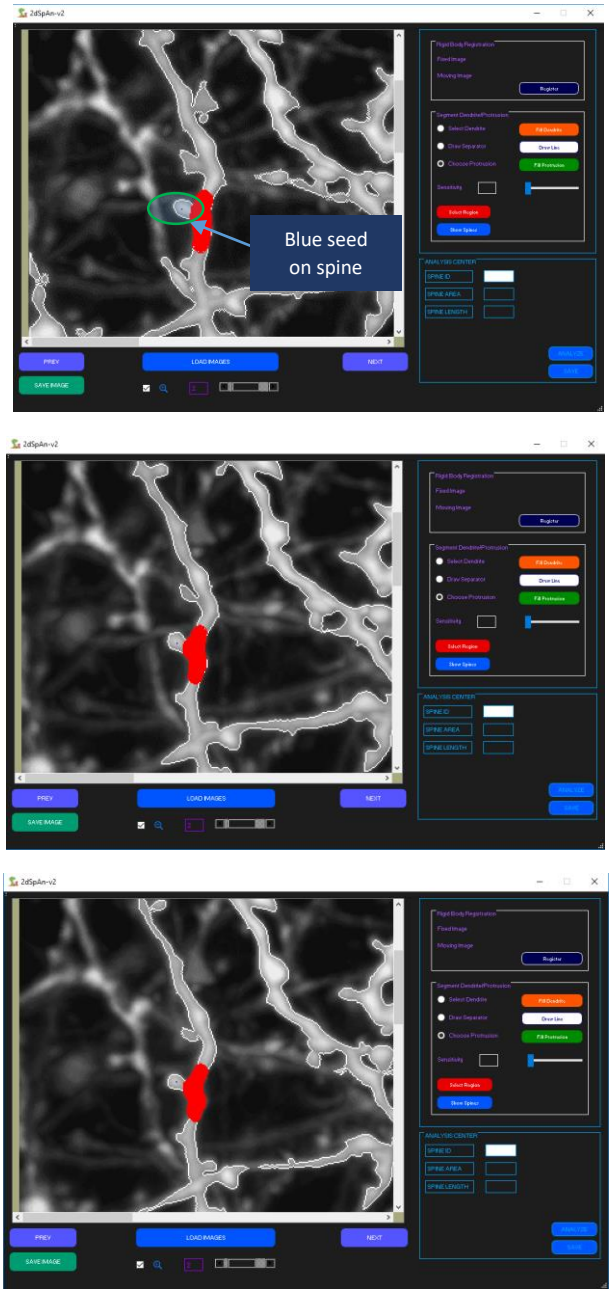

Fig 5.9 After the Choose radio button has been selected and on the T0 image spine is marked with blue point (a) Location of seed in T0 (b) Location of seed in T1 (c) Location of seed in T2

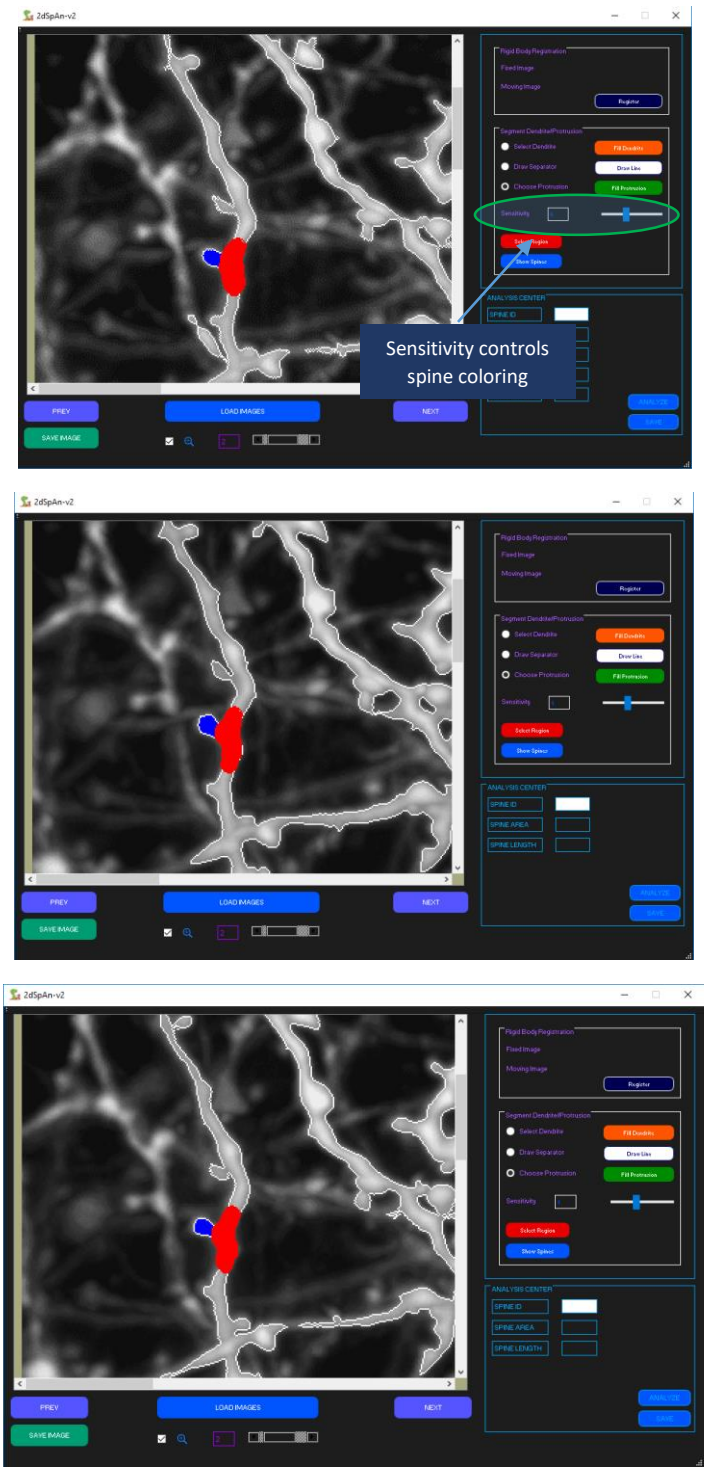

Fig 5.10 After the Fill Protrusion button has been clicked and spine segmentation has been done (a) Segmented spine in T0 (b) Segmented spine in T1 (c) Segmented spine in T2

5.3 EXPERIMENTAL RESULTS

The main purpose of our application 2DSpAn-v2 is to analyze dendritic spine plasticity in time series images. Both qualitative and quantitative analysis has been done on the images of dendritic spines from dissociated hippocampal cultures which have been obtained using confocal light microscopy. From the qualitative analysis we are able to visualize the changes in spine morphology by having a look at the time series images and from the quantitative analysis we are able to analyze and quantify changes in features like spine length, area, head-width, neck-length, etc. in time series images.

5.3.1 QUALITATIVE ANALYSIS

In the qualitative analysis of dendritic spines in time series images we are able to observe the morphological changes occurring in the dendritic spines. We have images of dendritic spines from dissociated hippocampal cultures 3 different time instants and from them the spines are segmented using our 2DSpAn-v2 application. The changes occurring in the shape of some of the dendritic spines over time instants T0, T1 and T2 is shown is figure 5.11.

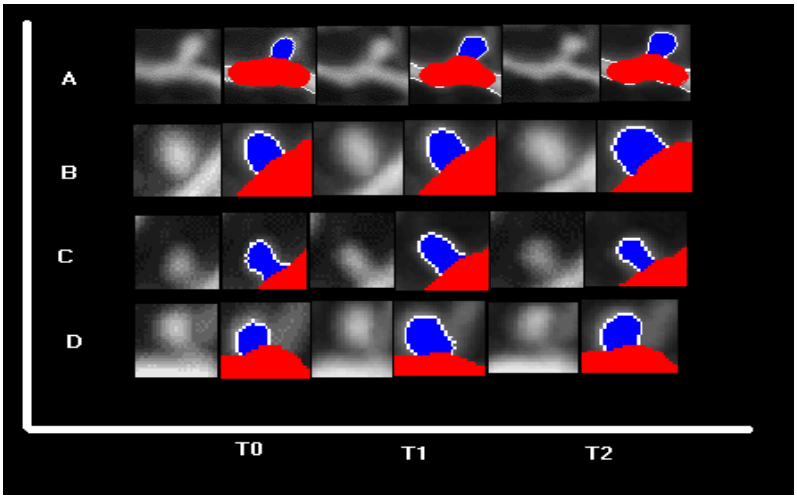

Fig 5.11 Segmented Spines and their morphological changes over time instants T0, T1 and T2.

5.3.2 QUANTITATIVE ANALYSIS

The morphology of the dendritic spines is complex and difficult to segment and quantify. In most cases, they are described by simple parameters like *length* and *area.* However, high resolution confocal microscopy allows visualization of the complex structures in greater details. In this work, we have attempted to define key morphological attributes from the

2D images of dendritic spines at different time instants. The figure 5.12 shows marked spines along with the features extracted in images of time stamps T0, T1 and T2 and the figure 5.13 shows the spine ID versus spine area and spine ID versus spine length in graphical representation.

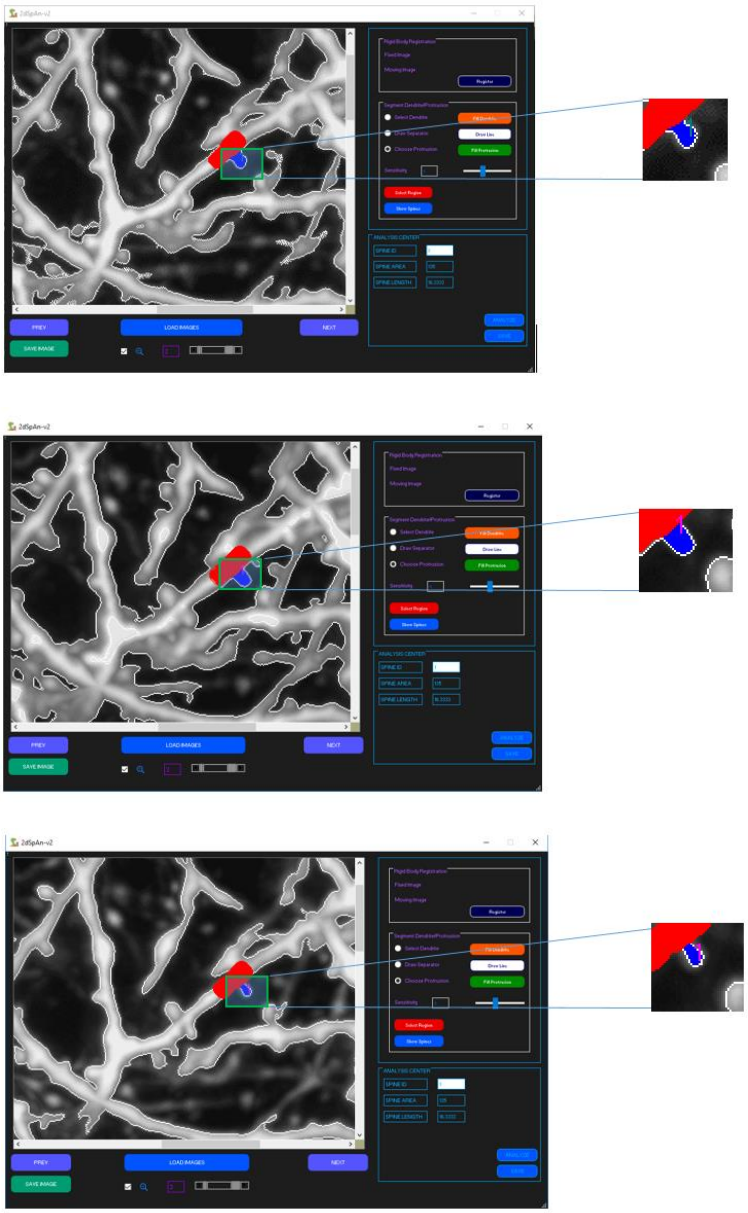

Fig 5.12 Marked spine in 2DSpAn-v2 GUI and quantitative feature extraction of marked spine at time instants T0, T1 and T2.

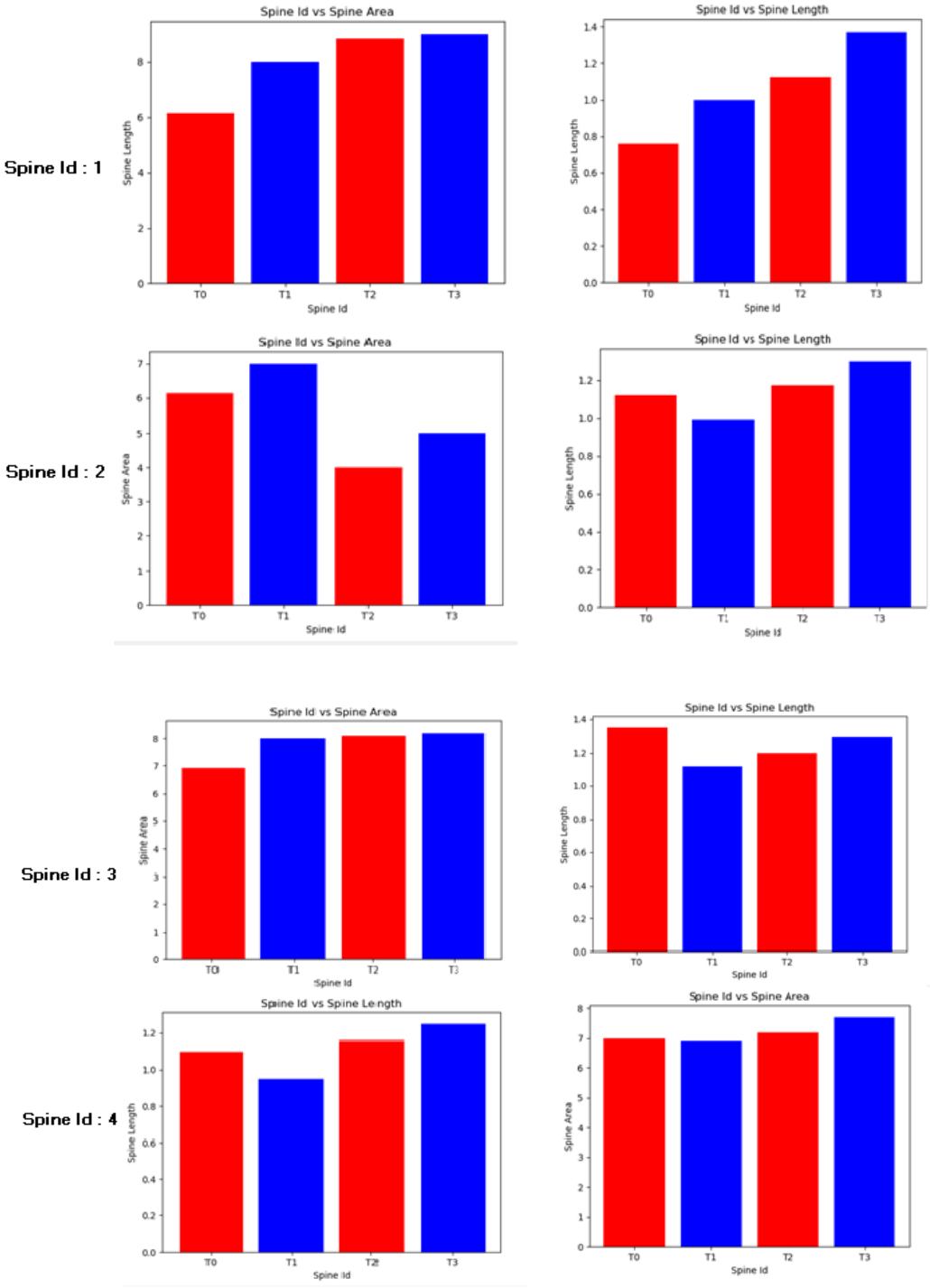

Fig 5.13 Graphs for Spine Id versus Spine Length and Spine Id versus Spine Area for Spine Id: 1, 2, 3, 4

CHAPTER 6

CONCLUSION

This thesis introduces the theory and algorithm of Quantitative Analysis of Dendritic Spine Plasticity using Image Registration in 2D MIP Images. Initially there is some sort of misalignment in the images of different time instants. Commonly, images are captured under variable conditions that might change the camera perspective or the scene's contents. Misalignment can also result from lens and sensor distortions or differences between capture devices. Image Registration helps to rectify this misalignment. So, firstly in the proposed 2DSpAn-v2 method the images are registered using our Image Registration method. Then, the segmentation of the dendrites and spines needs to be done. For dendrite segmentation the user needs to select two points on the region of interest and for the spine segmentation the user just needs to click on the concerned spine. We might have **N** number of images but we need to do these mouse events only on the image of the first timestamp and the segmentation automatically occurs for the remaining (N – 1) images. Since our main motive is plasticity analysis of spines in images of different time stamps so we compute features like spine length, spine area, etc. and display the results in our GUI. We review several methods of dendritic spine detection, reconstruction and analysis along with a brief discussion on some of the digital topology applications that can be used for better performance of spine analysis methods. From this we came to know although there are so many research works have been done so far in this area for 2D, 3D and 4D. But still there is a scope of improvement. These methods perform well in some extent but in every case, there are a lot of manual works needs to be done. Although the 2D-Span method required less human intervention but still some part of the tool needs manual point marking for selecting the region of interest. Our proposed method can be termed as **semi-automatic** and does give very good results for spine plasticity analysis.

Different experiment shows during highly stress or pathological condition spine dynamics unveil some anomalies like loss or decrease in spine numbers, immature structure of spine, reduction of size, highly variable spine density, ectopic spine formation, sometimes highly increased spine number .This method can be applicable to determine the spine morphology and changes in different stress model or in different pathological conditions like Alzheimer, Schizophrenia and Fragile X-syndrome (FXS). This can be used in different neuro-biological studies.

This method is tested only on different MIP images of confocal light microscopy and two-photon microscopy images of dendritic spines of rat dissociated hippocampal cultures. Due to the conversion of 3-D stack volume to 2-D using MIP some information may lost which may affect the performance of the algorithm. Some loop may be created after pre-processing as binarization fails to differentiate two different spines in some region where noisy pixels present due to 3-D to 2-D conversion.

In future, the work can be extended to do plasticity analysis of dendritic spines in 3-D as well. Other than that, in 2-D we need to improve our binarization algorithm that is more efficient in case of poor MIP images. The proposed registration algorithm performs quite well but due to the images being of very inferior quality binarization is an issue and therefore the performance of some tasks like Skeletonization, Segmentation of dendrite and spine, etc. can be improvised. This method only calculates the spine area and spine length in images of dendritic spines at different time instants. We can extend it to determine other features of individual spines like head width, neck length and classify them. We can reconstruct the whole dendritic spine from the skeleton in 3-D for better visualization.

References

[1] Filler A (12 July 2009). "The History, Development and Impact of Computed Imaging in Neurological Diagnosis and Neurosurgery: CT, MRI, and DTI". Nature Precedings. doi:10.1038/npre.2009.3267.5

[2] Sandrone S, Bacigaluppi M, Galloni MR, Martino G (November 2012). "Angelo Mosso (1846-1910)". Journal of Neurology. 259 (11): 2513–4. doi:10.1007/s00415-012-6632-1. PMID 23010944.

[3] Sandrone S, Bacigaluppi M, Galloni MR, Cappa SF, Moro A, Catani M, Filippi M, Monti MM, Perani D, Martino G (February 2014). "Weighing brain activity with the balance: Angelo Mosso's original manuscripts come to light". Brain. 137 (Pt 2): 621–33. doi:10.1093/brain/awt091

[4] Brown, C.; Li, P.; Boyd, J.; Delaney, K.; Murphy, T. (2007). "Extensive Turnover of Dendritic Spines and Vascular Remodeling in Cortical Tissues Recovering from Stroke". Journal of Neuroscience. 27 (15): 4101–4109. doi:10.1523/JNEUROSCI.4295-06.2007. PMID 17428988.

[5] Juan Carlos Stockert, Alfonso Blázquez-Castro (2017). "Chapter 6 Fluorescence Instrumental and Techniques". Fluorescence Microscopy in Life Sciences. Bentham Science Publishers. pp. 180–184. ISBN 978-1-68108-519-7. Retrieved 24 December 2017.

[6] Westphal, V.; S. O. Rizzoli; M. A. Lauterbach; D. Kamin; R. Jahn; S. W. Hell (2008). "Video-Rate Far-Field Optical Nanoscopy Dissects Synaptic Vesicle Movement". Science. 320 (5873): 246–249. Bibcode:2008Sci...320..246W. doi:10.1126/science.1154228. PMID 18292304

[7] Murphy, Gavin & Jensen, Grant. (2007). Electron Cryotomography. BioTechniques. 43. 413, 415, 417 passim. 10.2144/000112568.

[8] Pawley JB (editor) (2006). Handbook of Biological Confocal Microscopy (3rd ed.). Berlin: Springer. ISBN 0-387-25921-X.

[9] T. V. P. Bliss and T. Lømo, “Long-lasting potentiation of synaptic transmission in the dentate area of the anaesthetized rabbit following stimulation of the perforant path,” *J. Physiol.*, vol. 232, no. 2, pp. 331–356, 1973.

[10] A. Rusakov, T. V. P. Bliss, A. Fine, and M. Carlo, “Repeated Confocal Imaging of Individual Dendritic Spines in the Living Hippocampal Slice : Evidence for Changes in Length and Orientation Associated with Chemically Induced LTP,” vol. 75, no. August, 1995.

[11] M. Couprie and G. Bertrand, “New Characterizations of Simple Points in 2D , 3D , and 4D Discrete Spaces,” vol. 31, no. 4, pp. 637–648, 2009.

[12] M. Papa and M. Segal, “Morphological plasticity in dendritic spines of cultured hippocampal neurons,” *Neuroscience*, vol. 71, no. 4, pp. 1005–1011, 1996.

[13] J. J. Radley *et al.*, “Repeated stress induces dendritic spine loss in the rat medial prefrontal cortex,” *Cereb. Cortex*, vol. 16, no. 3, pp. 313–320, 2006.

[14] B. G. Kim, H. N. Dai, M. McAtee, S. Vicini, and B. S. Bregman, “Labeling of dendritic spines with the carbocyanine dye DiI for confocal microscopic imaging in lightly fixed cortical slices,” *J. Neurosci. Methods*, vol. 162, no. 1–2, pp. 237–243, 2007.

[15] V. A. Alvarez and B. L. Sabatini, “Anatomical and Physiological Plasticity of Dendritic Spines,” *Annu. Rev. Neurosci.*, vol. 30, no. 1, pp. 79–97, 2007.

[16] U. V. Nagerl, K. I. Willig, B. Hein, S. W. Hell, and T. Bonhoeffer, “Live-cell imaging of dendritic spines by STED microscopy,” *Proc. Natl. Acad. Sci.*, vol. 105, no. 48, pp. 18982–18987, 2008.

[17] J. Tønnesen, G. Katona, B. Rózsa, and U. V. Nägerl, “Spine neck plasticity regulates compartmentalization of synapses,” *Nat. Neurosci.*, vol. 17, no. 5, pp. 678–685, 2014.

[18] Y. Mishchenko, T. Hu, J. Spacek, J. Mendenhall, K. M. Harris, and D. B. Chklovskii, “Ultrastructural analysis of hippocampal neuropil from the connectomics perspective,” *Neuron*, vol. 67, no. 6, pp. 1009–1020, 2010.

[19] W. C. Oh, T. C. Hill, and K. Zito, “Synapse-specific and size-dependent mechanisms of spine structural plasticity accompanying synaptic weakening,” *Proc. Natl. Acad. Sci.*, vol. 110, no. 4, pp. E305–E312, 2013.

[20] R. Yuste, “Dendritic spines and distributed circuits,” *Neuron*, vol. 71, no. 5, pp. 772–781, 2011.

[21] R. Araya, T. P. Vogels, and R. Yuste, "Activity-dependent dendritic spine neck changes are correlated with synaptic strength," *Proc. Natl. Acad. Sci.*, vol. 111, no. 28, pp. E2895–E2904, 2014

[22] W. C. Risher, T. Ustunkaya, J. S. Alvarado, and C. Eroglu, "Rapid Golgi Analysis Method for Efficient and Unbiased Classification of Dendritic Spines," vol. 9, no. 9, 2014.

[23] S. Basu *et al.*, "2dSpAn: Semiautomated 2-d segmentation, classification and analysis of hippocampal dendritic spine plasticity," *Bioinformatics*, vol. 32, no. 16, pp. 2490–2498, 2016.

[24] B. Ruszczycki, J. Wlodarczyk, and L. Kaczmarek, "Method and a system for processing an image comprising dendritic spines." Google Patents, 08-Aug-2012.

[25] G. Naive and T. Worbs, "4D Tracking with Imaris," pp. 3–4.

[26] S. A. Swanger, X. Yao, C. Gross, and G. J. Bassell, "Automated 4D analysis of dendritic spine morphology : applications to stimulus-induced spine remodeling and pharmacological rescue in a disease model," *Mol. Brain*, vol. 4, no. 1, p. 38, 2011.

[27] P. Shi, Y. Huang, and J. Hong, "Automated three-dimensional reconstruction and morphological analysis of dendritic spines based on semi-supervised learning," vol. 5, no. 5, pp. 167–179, 2014.

[28] F. Janoos, K. Mosaliganti, X. Xu, R. Machiraju, K. Huang, and S. T. C. Wong, "Robust 3D reconstruction and identification of dendritic spines from optical microscopy imaging," *Med. Image Anal.*, vol. 13, no. 1, pp. 167–179, Feb. 2009.

[29] A. Rodriguez, D. B. Ehlenberger, D. L. Dickstein, P. R. Hof, and L. Susan, "Automated Three-Dimensional Detection and Shape Classification of Dendritic Spines from Fluorescence Microscopy Images," vol. 3, no. 4, 2008.

[30] S. Basu, P. K. Saha, M. Roszkowska, and M. Magnowska, "Quantitative 3-D morphometric analysis of individual dendritic spines," *Sci. Rep.*, no. February, pp. 1–13, 2018.

[31] S. Basu, P. K. Saha, E. Baczynska, M. Roszkowska, and M. Magnowska, "structural plasticity of hippocampal," no. March, 2018.

[32] P.A. van den Elsen, E-J.D. Pol, and M.A Viergiver. Medical Image Matching – a review with classification. IEEE Engineering in Medicine and Biology, 12(1):26-39, March 1993

[33] J.B.A Maintz and M.A. Viergever. A survey of medical image registration. Medical Image Analysis, 2(1):1-36, 1998.

[34] C. Nikou, F.Heitz, J-P. Armspach, and I-J. Namer. Single and multimodal subvoxel registration of dissimilar medical images using robust similarity measures. In *SPIE conference on Image Processing*, volume 3338, pages 167-178, San Diego, California, February 1998.

[35] A.Roche, G.Malandain, N.Ayache and S.Prima. Towards a better composition of similarity measures used in medical image registration. In Lecture notes in computer science pages, 555-66, Berlin, 999. Springer Verlag.

[36] W.M. Wells, P.Viola, H. Atsumi, S.Nakajima, and R.kikinis. Multimodal Volume Registration by maximization of mutual information. Medical Image Analysis, 1(1):35, 51, 1996.

[37] I.H. Habboush, K.D. Mitchell, R.V. Mulkern, P.D. Barnes, and S.T. Treves. Registration and alignment of three-dimensional images: An iterative visual approach. Radiology, 199(2)573-578, 1996.

[38] H. Blum and R. N. Nagel, "Shape description using weighted symmetric axis features," *Pattern Recognit.*, vol. 10, no. 3, pp. 167–180, 1978.

[39] G. S. di Baja, "Well-shaped, stable, and reversible skeletons from the (3, 4)-distance transform," *J. Vis. Commun. Image Represent.*, vol. 5, no. 1, pp. 107–115, 1994.

[40] D. Jin and P. K. Saha, "A new fuzzy skeletonization algorithm and its applications to medical imaging," in *International Conference on Image Analysis and Processing*, 2013, pp. 662–671.

[41] G. Borgefors, "Distance transformations in arbitrary dimensions," *Comput. Vision, Graph. Image Process.*, vol. 27, no. 3, pp. 321–345, 1984.

[42] L.G. Brown. A survey of Image Registration techniques. ACM Computing Surveys, 24(4):325-376, December 1992.

[43] N.Ayache Medical Computer Vision, virtual reality and robotics. Image and Vision Computing, 13(4):295-313, May 1995

[44] R.Bajscy and S.Kovacic. Multiresolution elastic matching. Computer Vision Graphics, and Image Processing, 46:1-21, 1989

[45] J.Banks. Reliability Analysis of Transform-Based Stereo Matching Techniques, and a new Matching constraint. PhD thesis, SCSN, School of Electrical and Electronic Systems Engineering, Queensland University of Technology, September 1999.

[46] Maes, Frederik & Collignon, André & Vandermeulen, Dirk & Marchal, Guy & Suetens, Paul. (1996). Multi-modality image registration by maximization of mutualinformation. IEEE Trans. Med. Imaging. 16. 14-22. 10.1109/MMBIA.1996.534053..

[47] L. G. Nyul and J. K. Udupa, .Incorporating a Measure of Local Scale in Voxel-Based 3-D Image Registration,. *IEEE Transactions on Medical Imaging*, vol. 22, no. 2, pp. 228-237, 2003.

[48] J. P. Pluim, J. B. Maintz, and M. A. Viergever, .Mutual information matching and interpolation artifacts,. *Proceedings of SPIE Medical Imaging: Image Processing*, vol. 3, pp. 661.

[49] P. Viola and W. M. Wells III, .Alignment by maximization of mutual information,. *International Conference on Computer Vision*, E.Grimson, S. Shafer, A. Blake, and K. Sugihara, eds., pp. 16-23, IEEE Computer Society Press, Los Alamitos, CA, 1995.

[50] J. P. Pluim, J. B. Maintz, and M. A. Viergever, .Image Resistration by Maximization of Combined Mutual Information and Gradient Information,. *IEEE Transactions on Medical Imaging*, vol. 19, no. 8, pp. 809-814, 2000.

[51] H. Chen and P. K. Varshney, .Registration of Multimodal Brain Images: Some Experimental Results,. *Proceedings of SPIE Conference on Sensor Fusion: Architectures, Algorithms, and Applications VI*, Orlando, FL, 2002.

[52] L. Freire, and F. Godinho, .Registration by maximization of mutual information - a cross validation study,. *IEEE International Symposium on Bio-Informatics and Biomedical Engineering*, pp. 322-329, 2000.

[53] Xiang Gao and Sébastien Loriot and Andrea Tagliasacchi. Triangulated Surface Mesh Skeletonization. In *CGAL User and Reference Manual*. CGAL Editorial Board, 4.14 edition, 2019